UNIVERSAL WISER
PUBLISHER

Research Article

Mathematical Analysis of the Dynamics of COVID-19 in the Face of Vaccination in African Countries

Paustella Azokpota[1] [ID] **, Robinah Nalwanga[1]** [ID] **, Yvette Montcho[1]** [ID] **, Kassifou Traoré[1], Jonas Têlé Doumatè[1,2], Romain Glèlè Kakaï[1]*** [ID]

[1] Laboratory of Biomathematics and Forest Estimation, University of Abomey-Calavi, Cotonou, Benin
[2] Faculty of Science and Technology, University of Abomey-Calavi, Cotonou, Benin
 E-mail: romain.glelekakai@uac.bj

Abstract: (1) Background: The ongoing COVID-19 pandemic has posed significant global challenges; its impact in Africa, in particular, has been a subject of increasing concern. Vaccination against COVID-19 started in many African countries in 2020. Despite the remarkable progress made by a selected number of countries initiating vaccination campaigns in 2020, the global vaccination coverage against the targeted disease remains inadequate. This study aimed to assess the dynamics of COVID-19 in the face of vaccination in Africa. (2) Methods: We used an extended deterministic Susceptible-Exposed-Infectious-Recovered (SEIR)-type model stratified by vaccination status to mathematically analyze the effect of vaccination on the dynamics of COVID-19 in ten African countries, namely: Benin, Namibia, South Africa, Rwanda, Lybia, DRC, Nigeria, Algeria, Gabon and Kenya. We studied some basic properties of the model and derived the control and basic reproduction numbers R_c and R_0, respectively. We further utilized the Castillo-Chavez method to investigate the global stability of the model at the disease-free equilibrium point under the condition $R_c < 1$. In addition, we developed the expressions of the sensitivity and elasticity of the control reproduction number (R_c) with respect to vaccination coverage, level of adherence to control measures (ψ_u and ψ_v), infection probabilities, and relative infectiousness of different compartments of Infected. The model was fitted using cumulative daily COVID-19 case data corresponding to each country's third wave of the pandemic. The unknown parameters are estimated using the non-linear least square method. We used the resulting parameter values to compute the sensitivity and elasticity indices. (3) Results: The study demonstrates the importance of sustaining high vaccination coverage and control measures to mitigate COVID-19 transmission in Africa. Results identify vaccination rates and population compliance to control measures as most influential based on sensitivity analysis. (4) Conclusions: By generating evidence tailored to the African context, this research provides crucial insights to inform resource allocation and interventions to combat COVID-19, where needs are greatest.

Keywords: mechanistic model, pandemic, vaccination coverage, theoretical analysis, application, Africa

MSC: 34A12, 22B22

1. Introduction

Humanity has dealt with several diseases over the past years, but health has become, by far, extremely vulnerable in the world due to the most recent of these: SARS-CoV-2, a new strain of coronavirus that first surfaced in December 2019 in Wuhan, may lead to the Coronavirus Disease 2019 (COVID-19) [1]. COVID-19 patients, according to the medical corps, suffer from mild to intermediate breathing issues, fatigue, flu, fever, and so on. In many areas, the COVID-19 virus spread quickly from one person to another, and the World Health Organization reported it as a pandemic on March 11, 2020 [2]. If the first large-scale COVID-19 outbreaks occurred predominantly in high-income nations in Europe and North America, with more than 4,170,424 cases as of May 13, 2020, [3], the disease has since spread throughout Africa. We could count 8,986,322 cases and 174,211 deaths on July 5, 2023 [4]. The World Health Organization (WHO) released many guidelines that different nations followed to avoid spreading disease. Social distancing, wearing a mask, keeping rooms properly aired, avoiding crowds, and cleansing hands with an alcohol-based sanitizer or soap and water were among the Non-Pharmaceutical Interventions (NPIs) [5]. In Uganda, Kenya, Malawi, and Ghana, the containment measures to curtail transmission of COVID-19 included closing international airports, closing schools, freezing public and private transportation, prohibiting all extensive gathering activities, and implementing widespread lockdowns [6]. To reduce the spread of infection, quarantine, and isolation of confirmed COVID-19 cases were also introduced in South Africa, Rwanda, Benin, and Nigeria [6]. However, vaccines are the most efficient and cost-effective method of preventing and controlling infectious diseases [7]. The availability of vaccines has represented a unique opportunity to fight the COVID-19 disease. In the realm of infectious disease research, mathematical modeling has emerged as a powerful tool to understand the transmission dynamics of epidemics [8–10]. In this context, many scientific works have developed several models to analyze the effect of vaccination on COVID-19 dynamic [11, 12]. Li et al. [13] used a modified Susceptible-Exposed-Infectious-Recovered (SEIR) mathematical model to estimate the effect of age-specific vaccine allocation strategies to reduce the cumulative number of deaths and new infections. They found that priority vaccination to the youngest age group would reduce the number of new infections most, and priority vaccination to the middle and elderly age groups would reduce the deaths most. Using a similar model, another study from [14] reveals that the higher the vaccination rate, the lower the peak reached by confirmed cases and deaths. However, the model did not account for the combined effect of implementing the routine vaccination program with control measures.

Love et al. [15] came across this gap by providing a valuable tool to evaluate the allocation of a limited vaccine supply, especially in the context of reduced or relaxing NPI measures. Their results illustrate how COVID-19 dynamics decrease more effectively when vaccination deployment is paired with strong adherence to NPIs. In [16], the authors formulated classical and fractional-order SEIR models for COVID-19 and compared their dynamics and stability to provide insights into the utility of fractional calculus for epidemic modeling. It is found that the fractional model better captures fluctuating dynamics observed in COVID-19 data and suggests smaller basic reproduction numbers more in line with estimates.

Sivashankar et al. [17] introduced a COVID-19 mathematical model that incorporates the Caputo-Fabrizio fractional derivative and subjected it to analytical scrutiny. Utilizing eigenvalue methods, they conduct a comprehensive stability analysis of the model. The key findings indicated that the disease-free equilibrium becomes asymptotically stable when a defined reproduction number is below the critical threshold of 1. Conversely, the system exhibits an unstable endemic equilibrium if the reproduction number surpasses this threshold. However, there are certain limitations, including the simplicity of the model structure and the absence of data fitting and forecasting capabilities. Kumar et al. in [18] constructed and evaluated SEIR models for COVID-19 using different fractional derivatives and assessed their predictive performance to determine the optimal fractional modeling approach. The Atangana-Baleanu fractional model provided the most accurate predictions of the epidemic peak timing in Japan.

However, the results of these studies may not apply to African countries due to significant differences in the data reported. Factors influencing the pandemic's dynamics across Africa are multiple, including infection fatality ratios, limited access to physical health services, vaccine hesitancy, and low testing rates [19]. Since its evolution, many papers have also investigated COVID-19 in Africa [10, 20–22]. In 2023, the study by Ashraf et al. [23] developed an improved mathematical model incorporating fear effects on COVID-19 transmission and demonstrated the role of fear in slowing down the epidemic through model analysis and simulations. The model demonstrates that higher levels of fear slow down

COVID-19 transmission. Stability analysis provides thresholds related to fear for controlling outbreaks. Model fitting to data shows the significant role of fear-induced behavioural changes.

In the study conducted by Honfo et al. [24], a simple deterministic susceptible-infectious-recovered (SIR)-type model was employed to characterize the initial wave of the COVID-19 pandemic and provide future trend forecasts across the sixteen West African countries. The findings of the study revealed several noteworthy observations. Firstly, a relatively low proportion of susceptible individuals was observed in the region and across the different countries. Additionally, the detection rate of the disease was relatively low, except for specific countries such as Gambia, Cape Verde, Mauritania, and Ghana.

Another study by Yedomonhan et al. [25] focused on expanding a Susceptible-Infectious-Quarantined-Removed (SIQR) disease-opinion dynamics model to take into account the effects of prophylactic behaviors on COVID-19 dynamics. The proposed method estimates the basic and time-varying reproduction numbers, the peak infection size of new infections, and the final epidemic size. The results highlight that the initial proportion of individuals perceiving COVID-19 as a severe threat and that of the followers of prophylactic behaviors are decisive in controlling the disease's spread. However, the model failed to account for the vaccination program. Moreover, it didn't incorporate the exposed compartment, representing individuals who have contracted the disease but are not yet contagious. As a result, the model may not accurately reflect the dynamics of the disease. To address the gap mentioned above in the literature, this study expands upon the research conducted by Montcho et al. [26], which proposes a novel compartmental model that caters to non-pharmaceutical measures to analyze the dynamics of the COVID-19 pandemic with vaccination programs in Africa. However, stability analysis of the model by Montcho et al. [26] is missing. Moreover, sensitivity and elasticity analyses were performed empirically, limiting the generalization of the results obtained. Thus, the main objective of this paper is to perform a mathematical analysis of the model used by Montcho et al. [26] and to study its stability. We further extend the analysis conducted by Montcho et al. [26] to additional African countries that were not addressed and develop the expression of the sensitivity and elasticity of the reproduction number with respect to various factors.

This expansion in the geographic scope adds a new dimension to the existing body of work, providing a more comprehensive understanding of COVID-19 dynamics in a total of ten African nations corresponding to different African regions and offering region-specific insights into COVID-19 dynamics. By acknowledging and incorporating these region-specific nuances, the research transcends generic analyses and furnishes a tailored perspective on the multifaceted dynamics of COVID-19 in diverse African nations. Furthermore, the application of the Castillo-Chavez method to assess global stability in a complex system characterized by multiple variables and substantial matrices adds a significant dimension to the work. This achievement highlights the research's ability to navigate the intricacies of large-scale epidemiological models, making it especially relevant in real-world scenarios. With the proposed model, we aim to (i) evaluate the effect of vaccination on incidences and mortality due to COVID-19 and (ii) assess the effect of vaccination on COVID-19 dynamics with different Non-Pharmaceutical intervention (NPIs) levels implemented.

The presentation of the work is structured as follows: The next section provides a detailed exposition of the compartmental SEIR model framework used to analyze the COVID-19 transmission dynamics model, including the underlying differential equations and model parameters. In the Results section, the research presents basic model properties as well as the basic and control reproduction numbers and assesses the global stability of the disease-free equilibrium. A comprehensive sensitivity and elasticity analysis examines the effect of some parameters on the model's dynamics, alongside a sensitivity analysis of incidences and mortalities. The research culminates with a discussion and conclusion.

2. Methods

In this study, we consider a compartmental mathematical model that was previously developed by Montcho et al. [26] to describe the dynamics of COVID-19 transmission in Africa. The proposed model is a modified SEIR model incorporating vaccination and control measures. The interacting human population, $N(t)$ at the time t, is divided into two subgroups, i.e. vaccinated and unvaccinated, represented by subscript u and v, respectively. That is

$N(t) = N_u(t) + N_v(t)$. The subpopulation of unvaccinated people, $N_u(t)$, was split into seven (7) compartments that are: Susceptible ($S_u(t)$), Exposed ($E_u(t)$), Pre-symptomatically infectious ($I_{Pu}(t)$), asymptomatically infectious ($I_{Au}(t)$), Symptomatically infectious ($I_{Su}(t)$), Confirmed cases ($C_u(t)$) and Recovered ($R_u(t)$). In addition, we consider the class $D_u(t)$, which comprises the unvaccinated individuals who die due to COVID-19-related complications.

$$N_u(t) = S_u(t) + E_u(t) + I_{Pu}(t) + I_{Au}(t) + I_{Su}(t) + C_u(t) + R_u(t). \tag{1}$$

The subpopulation of vaccinated individuals $N_v(t)$ is also divided into seven (7) compartments: Susceptible $S_v(t)$, Exposed $E_v(t)$, Pre-symptomatically infectious $I_{Pv}(t)$, Asymptomatically infectious $I_{Av}(t)$, Symptomatically infectious $I_{Sv}(t)$, confirmed individuals $C_v(t)$, recovered $R_v(t)$. Similarly, as for the previous group, we define $D_v(t)$ as the vaccinated people who died of COVID-19 disease.

$$N_v(t) = S_v(t) + E_v(t) + I_{Pv}(t) + I_{Av}(t) + I_{Sv}(t) + C_v(t) + R_v(t). \tag{2}$$

At any given time t, the unvaccinated and vaccinated people who die due to COVID-19-related complications that are $D_u(t)$ and $D_v(t)$ are not included in the interacting population $N_u(t)$ and $N_v(t)$. The state variables of the model are described in Table 1.
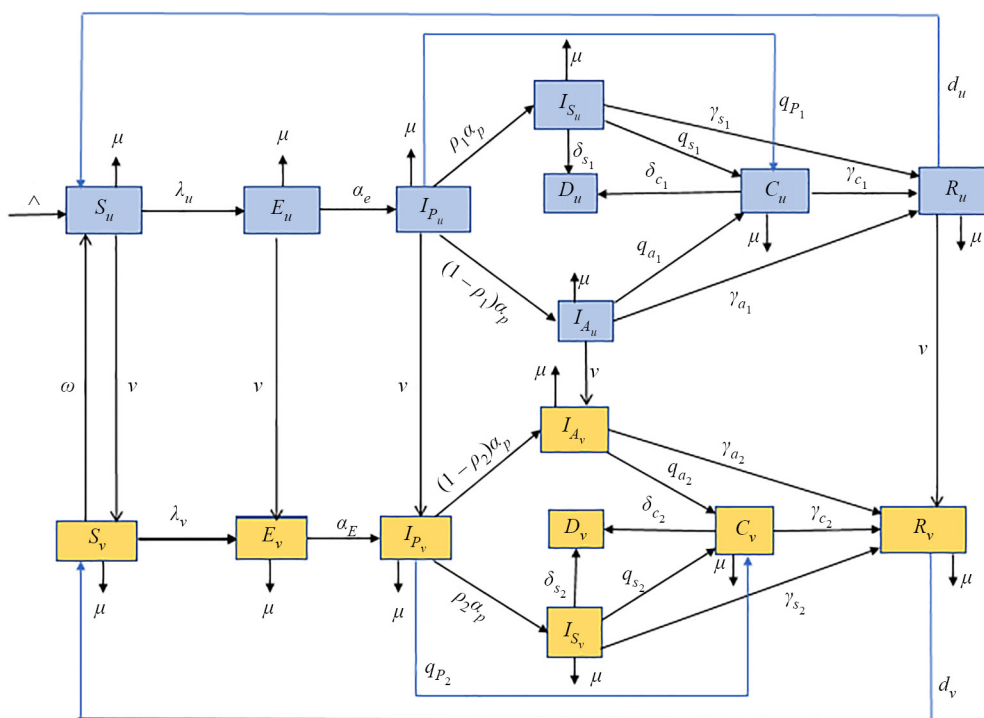
Table 1. Model compartment's description

State Variables	Description
$S_u(S_v)$	Susceptible unvaccinated (vaccinated) population that is non-infected yet. They can get vaccinated or exposed.
$E_u(E_v)$	Unvaccinated (vaccinated) population of exposed individuals. They are newly infected, do not show any symptoms and can't infect others.
$I_{P_u}(I_{P_v})$	Unvaccinated (vaccinated) pre-asymptomatic people: Exposed individuals who can (after the latent period) start infecting. They transit later to the asymptomatic or symptomatic class after the incubation period.
$I_{A_u}(I_{A_u})$	Unvaccinated (vaccinated) asymptomatic infectious population: these continue to show no symptoms of the disease after the incubation period.
$I_{S_u}(I_{S_v})$	Unvaccinated (vaccinated) symptomatic infectious population: people who start showing symptoms of the disease after the incubation period.
$C_u(C_v)$	Unvaccinated (vaccinated) confirmed cases: individuals who have been tested and confirmed positive for COVID-19.
$R_u(R_v)$	Unvaccinated (vaccinated) population of recovered individuals. They are no longer infected by the disease and can be susceptible again after losing natural immunity.
$D_u(D_v)$	Unvaccinated (vaccinated) population who died of COVID-19.

Source: Adapted from Montcho et al. [26]

We adopted the assumption of homogeneous mixing, wherein each individual is presumed to have an equal probability of encountering and interacting with any other member of the community. This assumption aligns with the prevalent practice in numerous prior studies conducted in the field [10, 27]. We assume a natural mortality rate μ in all compartments and a recruitment rate Λ of susceptible individuals. A comprehensive assessment of the recruitment rate for vaccination necessitates the inclusion of not only natural births and immigration but also young adults who have met the age requirement for vaccination, which is set at 18 years and above in the African context. We suppose that all unvaccinated individuals in the compartments can be vaccinated at the same rate, ν, except those in the symptomatic infectious and

confirmed classes. When susceptible unvaccinated individuals make contact with pre-symptomatic, asymptomatic, or symptomatic infectious individuals, whether they have been vaccinated or not, the infection can occur at the rate of λ_u. Similarly, because the vaccine is considered imperfect, it only confers partial protection, which implies that vaccinated individuals can get the disease at the rate λ_v once in contact with an infected individual. Hence, those populations are considered exposed: they do not show symptoms and cannot infect others. After the latent period, they become pre-symptomatic infectious and infect susceptible individuals at the rate α_e. After the incubation period, they move on to either asymptomatic infectious category at the rate $(1 - \rho_1)\alpha_p$ and $(1 - \rho_2)\alpha_p$ respectively for the unvaccinated and vaccinated or symptomatically infectious at a rate $\rho_1\alpha_p$ ($\rho_2\alpha_p$). Alternatively, they can be tested positive and join the confirmed case respectively at the detection rate q_{p_1} (q_{p_2}). The asymptomatic infectious population continues to show no symptoms. Thus, either they end up as confirmed cases after testing at a rate q_{a_1} (q_{a_2}) or they recover at a rate of γ_{a_1} (γ_{a_2}). In a study carried out by Wang et al., it was demonstrated that within the cohort of asymptomatic individuals admitted to Dongxihu Fangcang Hospital in China, more than 90 percent of patients remained without the aggravation of illness throughout the follow-up period [28]. We, therefore, assume in the model that asymptomatic individuals don't develop severe disease or die due to COVID-19. We also assume that exposed and pre-asymptomatic people cannot die of the disease, since they do not show any symptoms. On the other hand, the unvaccinated (vaccinated) symptomatic infectious individuals can be tested positive and join the confirmed class at the rate q_{s_1} (q_{s_2}), die of the disease at the rate δ_{s_1} (δ_{s_2}) or recover at the rate γ_{s_1} (γ_{s_2}). The COVID-19 induced mortality rate for the confirmed class is δ_{c_1} (δ_{c_2}). Also, it is assumed that the disease doesn't confer permanent immunity; the recovered individuals may become susceptible again. Therefore, they may join the susceptible compartment at the rate d_u (d_v). Also, the vaccine immunity is not lifelong and thus wanes over time, which implies that the susceptible lose the vaccine-induced immunity and join the susceptible unvaccinated class at a rate ω. All the information discussed in this section draws upon the comprehensive study conducted by Montcho et al. [26].

Figure 1. Flow chart of the formulated mathematical model
Source: Montcho et al. [26]

Table 2. Description of the model parameters

Parameter	Description
b_{ij}	Infection probability of groups i and j per contact (i, $j \in [1, 2]$)
v	Vaccination rate
μ	Natural death rate
Λ	Recruitment rate
ω	Waning vaccine immunity rate
$\lambda_u (\lambda_v)$	Force of infection on the unvaccinated (vaccinated)
$\theta_{p_u} (\theta_{p_v})$	Relative infectiousness of pre-symptomatic infectious unvaccinated (vaccinated)
$\theta_{a_u} (\theta_{a_v})$	Relative infectiousness of asymptomatic infectious unvaccinated (vaccinated)
$\theta_{s_u} (\theta_{s_v})$	Relative infectiousness of symptomatic infectious unvaccinated (vaccinated)
$\theta_{c_u} (\theta_{c_v})$	Relative infectiousness of confirmed unvaccinated (vaccinated)
$1/\alpha_e$	Latent period (per day)
$1/\alpha_p$	Pre-symptomatic period (per day)
$\rho_1 (\rho_2)$	Probability of developing symptoms for the unvaccinated (vaccinated)
$q_{s_1} (q_{s_2})$	Per capita rate at which unvaccinated (vaccinated) from the symptomatic infectious class test positive
$q_{a_1} (q_{a_2})$	Per capita rate at which unvaccinated (vaccinated) from the asymptomatic infectious class test positive
$1/\gamma_{a_1} (1/\gamma_{a_2})$	Recovery rate of asymptomatic unvaccinated (vaccinated) cases (per day)
$1/\gamma_{c_1} (1/\gamma_{c_2})$	Recovery rate of confirmed unvaccinated (vaccinated) cases (per day)
$d_u (d_v)$	Rate at which recovered unvaccinated (vaccinated) individuals from COVID-19 lose acquired natural immunity
$\delta_{s_1} (\delta_{s_2})$	COVID-19 death rate of symptomatic infectious unvaccinated (vaccinated) individuals
$\delta_{c_1} (\delta_{c_2})$	COVID-19 death rate of confirmed infectious unvaccinated (vaccinated) individuals

Source: Montcho et al. [26]

The schematic diagram of the model is shown in Figure 1 as well as an overall description of the parameters in Table 2. The transfer rates between compartments are expressed mathematically throughout the following non-linear differential equations in (3) and (4), respectively, for the unvaccinated and vaccinated population. A dot represents differentiation with respect to time t.

$$\dot{S}_u = \Lambda - (\lambda_u + \mu + v) S_u + d_u R_u + \omega S_v$$

$$\dot{E}_u = S_u \lambda_u - (\alpha_e + v + \mu) E_u,$$

$$\dot{I}_{P_u} = \alpha_e E_u - (\alpha_p + \mu + v + q_{p_1}) I_{P_u},$$

$$\dot{I}_{A_u} = (1 - \rho_1) \alpha_p I_{P_u} - (\mu + v + \gamma_{a_1} + q_{a_1}) I_{A_u},$$

$$\dot{I}_{S_u} = \rho_1 \alpha_p I_{P_u} - (\mu + \gamma_{s_1} + q_{s_1} + \delta_{s_1})I_{S_u},$$

$$\dot{C}_u = q_{a_1} I_{A_u} + q_{s_1} I_{S_u} + q_{p_1} I_{P_u} - (\delta_{c_1} + \gamma_{c_1} + \mu)C_u,$$

$$\dot{D}_u = \delta_{s_1} I_{S_u} + \delta_{c_1} C_u,$$

$$\dot{R}_u = \gamma_{a_1} I_{A_u} + \gamma_{s_1} I_{S_u} + \gamma_{c_1} C_u - (d_u + \mu + \nu)R_u, \tag{3}$$

$$\dot{S}_v = \nu S_u + d_v R_v - (\lambda_v + \mu + \omega)S_v,$$

$$\dot{E}_v = \nu E_u + S_v \lambda_v - (\alpha_e + \mu)E_v,$$

$$\dot{I}_{P_v} = \nu I_{P_u} + \alpha_e E_v - (\alpha_p + \mu + q_{p_2})I_{P_v},$$

$$\dot{I}_{A_v} = \nu I_{A_u} + (1 - \rho_2)\alpha_p I_{P_v} - (\mu + \gamma_{a_2} + q_{a_2})I_{a_v},$$

$$\dot{I}_{S_v} = \rho_2 \alpha_p I_{P_v} - (\mu + \gamma_{s_2} + q_{s_2} + \delta_{s_2})I_{S_v},$$

$$\dot{C}_v = q_{a_2} I_{A_v} + q_{s_2} I_{S_v} + q_{p_2} I_{P_v} - (\delta_{c_2} + \gamma_{c_2} + \mu)C_v,$$

$$\dot{D}_v = \delta_{s_2} I_{S_v} + \delta_{c_2} C_v,$$

$$\dot{R}_v = \nu R_u + \gamma_{a_2} I_{A_v} + \gamma_{s_2} I_{S_v} + \gamma_{c_2} C_v - (d_v + \mu)R_v. \tag{4}$$

The initial conditions are:

$$S_u(0) \geq 0; E_u(0) \geq 0; I_{P_u}(0) \geq 0; I_{A_u}(0) \geq 0; I_{S_u}(0) \geq 0;$$

$$C_u(0) \geq 0; D_u(0) \geq 0; R_u(0) \geq 0; S_v(0) \geq 0; E_v(0) \geq 0; I_{P_v}(0) \geq 0; I_{A_v}(0) \geq 0;$$

$$I_{S_v}(0) \geq 0; C_v(0) \geq 0; D_v(0) \geq 0; R_v(0) \geq 0.$$

The force of infection quantifies how much the infectious individuals can transmit the virus when they come in contact with the susceptible individuals in the population. The model's infectious compartments interacting with the susceptible individuals comprise the pre-symptomatic, asymptomatic, and symptomatic individuals. Even though the confirmed people are supposed to be isolated after testing positive and, therefore, do not make any contact with the susceptible, we still assume in this study that people tend not to respect this measure when the vaccination program has

begun fully. They might be mixed into the population and participate in the infection dynamic. This justifies why the confirmed compartment is also considered in the force of infection.

They might be mixed into the population and participate in the infection dynamic. This justifies why the confirmed compartment is also considered in the force of infection. We subdivide the overall force of infection into two: the force of infection rate λ_u and λ_v. λ_u quantifies how an infectious individual in the overall population can transmit the virus to unvaccinated susceptible individuals. Following the approach of Mancuso et al. [29], the force of infection rates λ_u is given by:

$$\lambda_u = \lambda_{uu} + \lambda_{vu} \tag{5}$$

where

$$\lambda_{uu} = \frac{(1 - \psi_u) b_{uu} \left(\theta_{p_u} I_{P_u} + \theta_{a_u} I_{A_u} + \theta_{s_u} I_{Su} + \theta_{c_u} C_u \right)}{N}$$

$$\lambda_{vu} = \frac{(1 - \psi_v) b_{vu} \left(\theta_{p_v} I_{P_v} + \theta_{a_v} I_{A_v} + \theta_{s_v} I_{S_v} + \theta_{c_v} C_v \right)}{N}.$$

The model accounts for implementing Non-Pharmaceutical Interventions that reduce this force of infection. ψ_u (ψ_v) is the proportion of unvaccinated (vaccinated) individuals who respect the control measures. On the other hand, b_{uu} is the infection probability of a susceptible individual in group 1 to get the disease per contact with an infectious individual in the same group. Also, in a mixed population of vaccinated and unvaccinated individuals, the susceptible individuals in group 1 are likely to make contact with individuals in group 2. If the contracting individual in group 2 is infectious, then the susceptible individual in group 1, S_u, is infected based on the probability b_{vu}. θ_{p_u}, θ_{a_u}, θ_{s_u} and θ_{c_u} are, respectively, the transmission rates of pre-symptomatic, asymptomatic, symptomatic infectious and confirmed unvaccinated. Similarly, θ_{p_v}, θ_{a_v}, θ_{s_v} and θ_{c_v} are respectively the transmission rates of pre-symptomatic, asymptomatic, symptomatic infectious and confirmed vaccinated. N is the total population, equivalently $N = N_u + N_v$.

Similarly, λ_v related to the capacity of an infectious individual in the overall population to transmit the virus to the vaccinated susceptible individuals is defined as follows:

$$\lambda_v = \lambda_{vv} + \lambda_{uv} \tag{6}$$

$$\lambda_{vv} = \frac{(1 - \psi_v) b_{vv} \left(\theta_{p_v} I_{P_v} + \theta_{a_v} I_{A_v} + \theta_{s_v} I_{S_v} + \theta_{c_v} C_v \right)}{N}$$

$$\lambda_{uv} = \frac{(1 - \psi_u) b_{uv} \left(\theta_{p_u} I_{P_u} + \theta_{a_u} I_{A_u} + \theta_{s_u} I_{S_u} + \theta_{c_u} C_u \right)}{N}.$$

On the other hand, b_{vv} is the infection probability of a susceptible individual in group 2 to get the disease per contact with an infectious individual in the same group. The susceptible individuals in group 2 are also likely to make contact with individuals in group 1. If the contracting individual in group 1 is infectious, then the susceptible individual in group 2, S_v, will be infected based on the probability b_{uv}.

3. Results

3.1 *Theoretical analysis of the model*

3.1.1 *Positiveness of the model solutions*

It is primordial for any mathematical model to show that the solutions of the system of equations are positive. In the following, we demonstrated that if the initial conditions of the system (3)-(4) are positive, then the solution set $S_u(t)$, $E_u(t)$, $I_{P_u}(t)$, $I_{A_u}(t)$, $I_{S_u}(t)(t)$, $C_u(t)$, $R_u(t)$, $D_u(t)$, $S_v(t)$, $E_v(t)$, $I_{P_v}(t)$, $I_{A_v}(t)$, $I_{S_v}(t)$, $C_v(t)$, $R_v(t)$, $D_v(t)$ of the model consists of positive members for all $t > 0$.

Referring to the differential equations in (3)-(4), we respectively have for:
- $S_u(t)$

$$\frac{dS_u}{dt} = \Lambda - (\lambda_u + \mu + v) S_u + d_u R_u + \omega S_v.$$

Then $\frac{dS_u}{dt} \geq \Lambda - (\lambda_u + \mu + v) S_u$ or $\frac{dS_u}{dt} + (\lambda_u + \mu + v) S_u \geq \Lambda$.
Multiplying each part of the inequality by $e^{(\lambda_u + \mu + v)t}$ gives:

$$[\frac{dS_u}{dt} + (\lambda_u + \mu + v) S_u] e^{(\lambda_u + \mu + v)t} \geq \Lambda e^{(\lambda_u + \mu + v)t},$$

$$\frac{dS_u}{dt} e^{(\lambda_u + \mu + v)t} + (\lambda_u + \mu + v) e^{(\lambda_u + \mu + v)t} S_u \geq \Lambda e^{(\lambda_u + \mu + v)t},$$

$$\frac{d}{dt}\left(S_u(t).e^{(\lambda_u + \mu + v)t}\right) \geq \Lambda e^{(\lambda_u + \mu + v)t},$$

$$\int_0^t \frac{d}{dy}\left(S_u(y).e^{(\lambda_u + \mu + v)y}\right) dy \geq \int_0^t \Lambda e^{(\lambda_u + \mu + v)y} dy,$$

$$\left[S_u(y).e^{(\lambda_u + \mu + v)y}\right]_0^t \geq \int_0^t \Lambda e^{(\lambda_u + \mu + v)y} dy,$$

$$S_u(t).e^{(\lambda_u + \mu + v)t} - S_u(0) \geq \int_0^t \Lambda e^{(\lambda_u + \mu + v)y} dy,$$

$$S_u(t).e^{(\lambda_u + \mu + v)t} \geq S_u(0) + \int_0^t \Lambda e^{(\lambda_u + \mu + v)y} dy,$$

$$S_u(t) \geq e^{-(\lambda_u + \mu + v)t}\left(S_u(0) + \int_0^t \Lambda e^{(\lambda_u + \mu + v)y} dy\right) > 0.$$

Hence, $S_u(t)$ is positive for $t > 0$.
- $E_u(t)$

With the second equation, we got the inequality $\frac{dE_u}{dt} + (\alpha_e + v + \mu) E_u \geq 0$.
Solving the equation $\frac{dE_u}{dt} + (\alpha_e + v + \mu) E_u = 0$ gives $E_u(t) = E_u(0) e^{-(\alpha_e + v + \mu)t} > 0$.
Hence, $E_u(t)$ is positive for all $t > 0$.

From the remaining equations of the system (3)-(4), it can be shown that the set of the solutions is positive for all $t > 0$. with the same process.

3.1.2 *Boundedness of the model solutions*

The overall population $N(t)$ is defined by adding both expressions in equations (1) and (2). Differentiating both sides with respect to t, we have:

$$\dot{N} = \dot{S}_u + \dot{E}_u + \dot{I}_{P_u} + \dot{I}_{A_u} + \dot{I}_{S_u} + \dot{C}_u + \dot{R}_u + \dot{S}_v + \dot{E}_v + \dot{I}_{P_v} + \dot{I}_{A_v} + \dot{I}_{S_v} + \dot{C}_v + \dot{R}_v. \tag{7}$$

Therefore,

$$\dot{N} = \Lambda - \mu N - (\delta_{s_2} I_{S_v} + \delta_{s_1} I_{S_u} + \delta_{s_2} C_v + \delta_{s_1} C_u). \tag{8}$$

That is,

$$\dot{N} \leq \Lambda - \mu N. \tag{9}$$

After integration, we get: $N(t) \leq N(0)e^{-\mu t} + \frac{\Lambda}{\mu}(1 - e^{-\mu t})$.

Hence, as $t \to \infty$, $N(t) \leq \frac{\Lambda}{\mu}$. Then, all solutions of the system enter into the region Ω with

$\Omega = \{(S_u, E_u, I_{P_u}, I_{A_u}, I_{S_u}, C_u, R_u, S_v, E_v, I_{P_v}, I_{A_v}, I_{S_v}, C_v, R_v) \in \mathbb{R}_+^{14} : 0 < N(t) \leq \Lambda/\mu\}$.

3.1.3 *Control reproduction number*

In disease modeling, the control reproduction number, R_c, is a key parameter used to assess the extent to which the pandemic will spread. The control reproduction number of an infectious agent, such as the coronavirus, is computed when the control measures and/or vaccination programs are implemented [30]. It is defined as the average number of secondary infections generated by one infectious individual when introduced in a mixed population consisting of vaccinated and unvaccinated individuals. When the control reproduction number R_c is less than one, each infected individual, vaccinated or not, infects less than one susceptible individual. This suggests that the virus will gradually be eradicated from the population. Otherwise, when R_c is greater than one, the number of COVID-19 cases caused by an infected individual increases exponentially over time, resulting in a growing epidemic.

From the studies, R_c is determined as the dominant eigenvalue of the next-generation matrix $\mathbf{FV}^{-1}$ where $\mathbf{F}$ and $\mathbf{V}$ are the jacobian of the matrix F of all the new infections and the matrix V of the net transition rates of compartments, respectively. [31, 32]. In the following study, we used the same approach.

Let $\mathrm{x} = (E_u, I_{P_u}, I_{A_u}, I_{S_u}, C_u, E_v, I_{P_v}, I_{A_v}, I_{S_v}, C_v)^{\mathrm{T}}$ be the vector of all the infected compartments. F and V are defined as follows:

$$F(x) = \begin{pmatrix} \lambda_u S_u \\ 0 \\ 0 \\ 0 \\ 0 \\ \lambda_v S_v \\ 0 \\ 0 \\ 0 \\ 0 \end{pmatrix} \quad \text{and} \quad V(x) = \begin{pmatrix} (\alpha_e + \nu + \mu)E_u \\ -\alpha_e E_u + (\alpha_p + \mu + \nu + q_{p_1})I_{P_u} \\ -(1-\rho_1)\alpha_p I_{P_u} + (\mu + \nu + \gamma_{a_1} + q_{a_1})I_{A_u} \\ -\rho_1 \alpha_p I_{P_u} + (\mu + \gamma_{s_1} + q_{s_1} + \delta_{s_1})I_{S_u} \\ (\delta_{e1} + \gamma_{c1} + \mu)C_u - q_{a1}I_{A_u} - q_{p1}I_{P_u} - q_{s1}I_{S_u} \\ -\nu E_u + (\alpha_e + \mu)E_v \\ -\nu I_{P_u} - \alpha_e E_v + (\alpha_p + \mu + q_{p_2})I_{P_v} \\ -\nu I_{A_u} - (1-\rho_2)\alpha_p I_{P_v} + (\mu + \gamma_{a_2} + q_{a_2})I_{a_v} \\ -\rho_2 \alpha_p I_{P_v} + (\mu + \gamma_{s_2} + q_{s_2} + \delta_{s_2})I_{S_v} \\ -q_{a_2}I_{A_v} - q_{p_2}I_{P_v} - q_{s_2}I_{S_v} + (\delta_{c_2} + \gamma_{c_2} + \mu)C_v \end{pmatrix}.$$

Hence, the jacobian matrices **F** and **V** are 10×10 matrices. In a disease-free state, only the susceptible classes are non-empty since there is no disease. Then:

$$(S_u, E_u, I_{P_u}, I_{A_u}, I_{S_u}, C_u, R_u, D_u, S_v, E_v, I_{P_v}, I_{A_v}, I_{S_v}, C_v, R_v, D_v)$$

$$= (S_u^0, 0, 0, 0, 0, 0, 0, 0, S_v^0, 0, 0, 0, 0, 0, 0, 0)$$

with $S_u^0 = \frac{\lambda(\mu+\omega)}{\mu(\nu+\mu+\omega)}$, and $S_v^0 = \frac{\Lambda \nu}{\mu(\nu+\mu+\omega)}$.

$$\mathbf{F(x)} = \begin{bmatrix} F_{11} & F_{12} \\ F_{21} & F_{22} \end{bmatrix} \text{with,}$$

$$F_{11} = \begin{bmatrix} 0 & \frac{S_u^0 b_{uu}\theta_{pu}(1-\psi_u)}{N^0} & \frac{S_u^0 b_{uu}\theta_{au}(1-\psi_u)}{N^0} & \frac{S_u^0 b_{uu}\theta_{su}(1-\psi_u)}{N^0} & \frac{S_u^0 b_{uu}\theta_{cu}(1-\psi_u)}{N^0} \\ 0 & 0 & 0 & 0 & 0 \\ 0 & 0 & 0 & 0 & 0 \\ 0 & 0 & 0 & 0 & 0 \\ 0 & 0 & 0 & 0 & 0 \end{bmatrix}$$

$$F_{12} = \begin{bmatrix} 0 & \frac{S_u^0 b_{vu}\theta_{pu}(1-\psi_v)}{N^0} & \frac{S_u^0 b_{vu}\theta_{au}(1-\psi_v)}{N^0} & \frac{S_u^0 b_{vu}\theta_{su}(1-\psi_v)}{N^0} & \frac{S_u^0 b_{vu}\theta_{cu}(1-\psi_v)}{N^0} \\ 0 & 0 & 0 & 0 & 0 \\ 0 & 0 & 0 & 0 & 0 \\ 0 & 0 & 0 & 0 & 0 \\ 0 & 0 & 0 & 0 & 0 \end{bmatrix}$$

$$F_{21} = \begin{bmatrix} 0 & \frac{S_v^0 b_{uv}\theta_{pu}(1-\psi_u)}{N^0} & \frac{S_v^0 b_{uv}\theta_{au}(1-\psi_u)}{N^0} & \frac{S_v^0 b_{uv}\theta_{su}(1-\psi_u)}{N^0} & \frac{S_v^0 b_{uv}\theta_{cu}(1-\psi_u)}{N^0} \\ 0 & 0 & 0 & 0 & 0 \\ 0 & 0 & 0 & 0 & 0 \\ 0 & 0 & 0 & 0 & 0 \\ 0 & 0 & 0 & 0 & 0 \end{bmatrix}$$

$$F_{22} = \begin{bmatrix} 0 & \frac{S_v^0 b_{vv}\theta_{pu}(1-\psi_v)}{N^0} & \frac{S_v^0 b_{vv}\theta_{au}(1-\psi_v)}{N^0} & \frac{S_v^0 b_{vv}\theta_{su}(1-\psi_v)}{N^0} & \frac{S_v^0 b_{vv}\theta_{cu}(1-\psi_v)}{N^0} \\ 0 & 0 & 0 & 0 & 0 \\ 0 & 0 & 0 & 0 & 0 \\ 0 & 0 & 0 & 0 & 0 \\ 0 & 0 & 0 & 0 & 0 \end{bmatrix}$$

N^0 is the initial population at disease-free equilibrium and is given by $N^0 = S_u^0 + S_v^0$.

$$\mathbf{V(x)} = \begin{bmatrix} a_1 & 0 & 0 & 0 & 0 & 0 & 0 & 0 & 0 & 0 \\ -\alpha_e & a_2 & 0 & 0 & 0 & 0 & 0 & 0 & 0 & 0 \\ 0 & \alpha_p(\rho_1-1) & a_3 & 0 & 0 & 0 & 0 & 0 & 0 & 0 \\ 0 & -\rho_1\alpha_p & 0 & a_4 & 0 & 0 & 0 & 0 & 0 & 0 \\ 0 & -q_{p_1} & -q_{a_1} & -q_{s_1} & a_5 & 0 & 0 & 0 & 0 & 0 \\ -\nu & 0 & 0 & 0 & 0 & a_6 & 0 & 0 & 0 & 0 \\ 0 & -\nu & 0 & 0 & 0 & -\alpha_e & a_7 & 0 & 0 & 0 \\ 0 & 0 & -\nu & 0 & 0 & 0 & -\alpha_p(1-\rho_2) & a_8 & 0 & 0 \\ 0 & 0 & 0 & 0 & 0 & 0 & -\rho_2\alpha_p & 0 & a_9 & 0 \\ 0 & 0 & 0 & 0 & 0 & 0 & -q_{p_2} & -q_{a_2} & -q_{s_2} & a_0 \end{bmatrix} \quad \text{with;}$$

$$a_1 = \alpha_e + \nu + \mu;$$

$$a_2 = \alpha_p + \nu + \mu + q_{p_1};$$

$$a_3 = \gamma_{a_1} + \nu + \mu + q_{a_1};$$

$$a_4 = \delta_{s_1} + \gamma_{s_1} + \mu + q_{s_1};$$

$$a_5 = \delta_{c_1} + \gamma_{c_1} + \mu;$$

$$a_6 = \alpha_e + \mu;$$

$$a_7 = \alpha_p + \mu + q_{p_2};$$

$$a_8 = \gamma_{a_2} + \mu + q_{a_2};$$

$$a_9 = \delta_{s_2} + \gamma_{s_2} + \mu + q_{s_2};$$

$$a_0 = \gamma_{c_2} + \delta_{c_2} + \mu.$$

The control reproduction number R_c is computed as the spectral radius $\boldsymbol{\rho}\left(\mathbf{F} \times \mathbf{V}^{-1}\right)$ of the next generation matrix, i.e.

$$R_c = \boldsymbol{\rho}\left(\mathbf{F} \times \mathbf{V}^{-1}\right).$$

Let's define:

$$R_c = R_{c_1} + R_{c_2} + R_{c_3}. \tag{10}$$

We split the Control reproduction number into three contributions. R_{c_1} is the contribution of the pre-symptomatic, asymptomatic, symptomatic and confirmed infectious unvaccinated people, respectively, to the control reproduction number; R_{c_2}, the contribution of the pre-symptomatic, asymptomatic, symptomatic and confirmed infectious vaccinated people respectively, and R_{c_3}, the contribution of the interaction of the vaccinated and unvaccinated infectious classes. We have:

$$R_{c_1} = R_{c_{1Pu}} + R_{c_{1Au}} + R_{c_{1Su}} + R_{c_{1Cu}} \tag{11}$$

where,

$$R_{c_{1Pu}} = \frac{\alpha_e S_u^0 b_{uu}(1-\psi_u)\theta_{p_u}}{2N^0 a_1 a_2};$$

$$R_{c_{1Au}} = \frac{\alpha_e S_u^0 b_{uu}(1-\psi_u)\alpha_p(1-\rho_1)\theta_{a_u}}{2N^0 a_1 a_2 a_3};$$

$$R_{c_{1Su}} = \frac{\alpha_e S_u^0 b_{uu}(1-\psi_u)\alpha_p \rho_1 \theta_{s_u}}{2N^0 a_1 a_2 a_4};$$

$$R_{c_{1Cu}} = \frac{\alpha_e S_u^0 b_{uu}(1-\psi_u)\left[a_3(a_4 q_{p_1} + q_{s_1}\rho_1 \alpha_p) + a_4 q_{a_1}\alpha_p(1-\rho_1)\right]\theta_{c_u}}{2N^0 a_1 a_2 a_3 a_4 a_5}.$$

Similarly, the component R_{c_2} is the sum of the four components $R_{c_{2Pv}}$, $R_{c_{2Av}}$, $R_{c_{2Sv}}$, and $R_{c_{2Cv}}$, which represent the contribution of the pre-asymptomatic, asymptomatic, symptomatic, and confirmed infectious vaccinated individuals, respectively. One has:

$$R_{c_2} = R_{c_{2Pv}} + R_{c_{2Av}} + R_{c_{2Sv}} + R_{c_{2Cv}} \qquad (12)$$

where,

$$R_{c_{2Pv}} = \frac{\alpha_e S_v^0 b_{vv}(1 - \psi_v)\theta_{p_v}}{2N^0 a_6 a_7};$$

$$R_{c_{2Av}} = \frac{\alpha_e S_v^0 b_{vv}(1 - \psi_v)\alpha_p(1 - \rho_2)\theta_{a_v}}{2N^0 a_6 a_7 a_8};$$

$$R_{c_{2Sv}} = \frac{\alpha_e S_v^0 b_{vv}(1 - \psi_v)\alpha_p \rho_2 \theta_{s_v}}{N^0 a_6 a_7 a_9};$$

$$R_{c_{2Cv}} = \frac{\alpha_e S_v^0 b_{vv}(1 - \psi_v)\left[a_8(a_9 q_{p_2} + q_{s_2}\alpha_p \rho_2) + a_9 q_{a_2}\alpha_p(1 - \rho_2)\right]\theta_{c_v}}{2N^0 a_0 a_6 a_7 a_8 a_9}.$$

Finally, the quantity, R_{c_3} is defined as:

$$R_{c_3} = R_{c_{1V}} + \sqrt{\left[R_{c_1} + R_{c_{1V}} - R_{c_2}\right]^2 + \frac{4R_{c_2}}{m_2}\left(m_1 R_{c_1} + m_2 R_{c_{1V}}\right)} \qquad (13)$$

where,

$$R_{c_{1V}} = R_{c_{1Pv}} + R_{c_{1Av}} + R_{c_{1Sv}} + R_{c_{1Cv}}, \; m_1 = \frac{b_{uv}}{b_{uu}}, \text{ and } m_2 = \frac{b_{vv}}{b_{vu}}.$$

We define $R_{c_{1V}}$ as the sum of four components, i.e. $R_{c_{1Pv}}$, $R_{c_{1Av}}$, $R_{c_{1Sv}}$, and $R_{c_{1Cv}}$, which represent the contribution from the interaction of the unvaccinated individuals with the pre-asymptomatic, symptomatic, and confirmed infectious vaccinated individuals. The components are defined as follows:

$$R_{c_{1Pv}} = \frac{\alpha_e v S_u^0 b_{vu}(1 - \psi_v)\theta_{p_v}}{2N^0 a_1 a_2 a_6 a_7};$$

$$R_{c_{1Av}} = \frac{\alpha_e v S_u^0 b_{vu}(1 - \psi_v)\left[a_3(1 - \rho_2)(a_2 + a_6 + a_6 a_7(1 - \rho_1))\right]\theta_{a_v}}{2N^0 a_1 a_2 a_3 a_6 a_7 a_8};$$

$$R_{c_{1Sv}} = \frac{\alpha_e v S_u^0 b_{vu}(1 - \psi_v)\alpha_p \rho_2(a_2 + a_6)\theta_{s_v}}{2N^0 a_1 a_2 a_6 a_7 a_9};$$

$$R_{c_{1Cv}} = \frac{\alpha_e v S_u^0 b_{vu}(1 - \psi_v)\left[a_3(a_2 + a_6)\left(a_8(a_9 q_{p_2} + \alpha_P q_{s_2}\rho_2) + a_9 \alpha_P q_{a_2}(1 - \rho_2)\right) + Z\right]\theta_{c_v}}{2N^0 a_0 a_1 a_2 a_3 a_6 a_7 a_8 a_9};$$

$$Z = a_9 a_6 a_7 q_{a_2} \alpha_P (1 - \rho_1).$$

3.1.4 *Basic reproduction number*

When no vaccination and non-pharmaceutical interventions are implemented, the disease's dynamic is measured by the Basic Reproduction number. In this case, the parameters related to vaccination rate and the decrease in the disease due to control strategies, respectively, v and $\psi_u(\psi_v)$, will be set to zero. That is $v = \omega = \psi_u = \psi_v = 0$. These values are replaced in the equation (10) to get the basic reproduction number R_0 given by the equation below.

$$R_0 = R_{0c_1} + R_{0c_2} + R_{0c_3}. \tag{14}$$

Thus, R_{0c1} represents the contribution of the pre-symptomatic, asymptomatic, symptomatic and confirmed infectious unvaccinated people, respectively, to the basic reproduction number. R_{0c3} is the contribution for the interaction of the vaccinated and unvaccinated infectious classes. By definition, R_{0c2} is equal to 0. Since we are in the absence of vaccination, there is no contribution of the infectious vaccinated people to the basic reproduction number $(S_v^0 = 0)$

$$R_{0c_1} = R_{0c_{1Pu}} + R_{0c_{1Au}} + R_{0c_{1Su}} + R_{0c_{1Cu}}$$

where,

$$R_{0c_{1Pu}} = \frac{\alpha_e b_{uu} \theta_{pu}}{2a_6(\alpha_p + \mu + q_{p_1})};$$

$$R_{0c_{1Au}} = \frac{\alpha_e \alpha_p b_{uu} \theta_{au} (1 - p_1)}{2a_6(\alpha_p + \mu + q_{p_1})(\gamma_{a_1} + \mu + q_{a_1})};$$

$$R_{0c_{1Su}} = \frac{\alpha_e \alpha_p b_{uu} \rho_1 \theta_{s_u}}{2a_4 a_6(\alpha_p + \mu + q_{p_1})};$$

$$R_{0c_{1Cu}} = \frac{\alpha_e b_{uu}(1 - \psi_u)\left[(\gamma_{a_1} + \mu + q_{a_1})a_4 + a_4 q_{a_1}\alpha_p(1 - \rho_1) + (\gamma_{a_1} + \mu + q_{a_1})q_{s_1}\rho_1\right]\theta_{c_u}}{2(\alpha_e + \mu)(\alpha_p + \mu + q_{p_1})(\gamma_{a_1} + \mu + q_{a_1})a_4 a_5}.$$

As well, the quantity, R_{0c_3} is also defined as;

$$R_{0c_3} = R_{0c_1}.$$

3.2 *Global stability analysis of the model*

The model stability is studied around the equilibrium points. There are usually two: the Disease Free Equilibrium (DFE) and Endemic Equilibrium Point (EEP). In the following, we only focused on the global stability analysis of the COVID-19 model (3)-(4) at the disease-free equilibrium. The global stability of the disease-free equilibrium holds

significant implications. Specifically, if the disease-free equilibrium is proven to be globally stable, the disease will not be able to remain in the population, regardless of the size of the perturbation. An influx of infected cases may cause a localized epidemic outbreak, but the disease won't become endemic in the population [33].

We used the Castillo-Chavez method [34] to prove that the model is globally asymptotically stable at the disease-free equilibrium. Considering the method of Castillo-Chavez, the COVID-19 model can be transformed as the following two subsystems:

$$\frac{dp_1}{dt} = Y_1(p_1, p_2);$$

$$\frac{dp_2}{dt} = Y_2(p_1, p_2).$$

where p_1 denotes the number of uninfected individuals; thus, $p_1 = (S_u, R_u, S_v, R_v)$, and p_2 represents the number of infected individuals, with, $p_2 = (E_u, I_{P_u}, I_{A_u}, I_{S_u}, C_u, S_v, E_v, I_{P_v}, I_{A_v}, I_{S_v}, C_v)$. The disease-free equilibrium point is given by $P_o = (p_1^0, 0)$.

The point $(Y_1^0, 0)$ is a globally stable asymptotically stable equilibrium for the model (3)-(4) provided $R_c < 1$, if the below criteria are satisfied.

1. Given $\frac{dp_1}{dt} = Y_1(p_1, 0)$, (p_1^0) is globally asymptotically stable.

2. $Y_2(p_1, p_2) = B.p_2 - \hat{Y}_2(p_1, p_2)$, where $\hat{Y}_2(p_1, p_2) \geq 0$ for $(p_1, p_2) \in \Omega$ and is B the Jacobian matrix of $Y_2(p_1, p_2)$ at the disease free equilibrium with positive off-diagonal entries.

If the model Equation meets the above conditions; then, the following theorem holds.

Theorem 1 The point $P_o = (p_1^0, 0)$ is globally asymptotically stable equilibrium provided $R_c < 1$ and the conditions 1. and 2. are satisfied.

Proof. Let $p_1 = (S_u, R_u, S_v, R_v)$ and $p_2 = (E_u, I_{P_u}, I_{A_u}, I_{S_u}, C_u, S_v, E_v, I_{P_v}, I_{A_v}, I_{S_v}, C_v)$, and define $P_o = (p_1^0, 0)$, where $p_1^0 = (S_u^0, R_u^0, S_v^0, R_v^0)$.

By using model system (3)-(4), we have:

$$\frac{dp_1}{dt} = \begin{pmatrix} \Lambda - (\lambda_u + \mu + \nu)S_u + d_u R_u + \omega S_v \\ \gamma_{a_1} I_{A_u} + \gamma_{s_1} I_{S_u} + \gamma_{c_1} C_u - (d_u + \mu + \nu)R_u \\ \nu S_u + d_\nu R_\nu - (\lambda_\nu + \mu + \omega)S_\nu \\ \nu R_u + \gamma_{a_2} I_{A_\nu} + \gamma_{s_2} I_{S_\nu} + \gamma_{c_2} C_\nu - (d_\nu + \mu)R_\nu \end{pmatrix} \quad \text{and;} \quad Y_1(p_1, 0) = \begin{pmatrix} \Lambda - (\mu + \nu)S_u + d_u R_u + \omega S_v \\ -(d_u + \mu + \nu)R_u \\ \nu S_u + d_\nu R_\nu - (\mu + \omega)S_\nu \\ \nu R_u - (d_\nu + \mu)R_\nu \end{pmatrix}.$$

Solving the equation $\frac{dp_1}{dt} - Y_1(p_1, 0) = 0$, partially gives, $R_u(t) = R_u(0)e^{-(d_u + \mu + \nu)t}$.

$R_\nu'(t) = K_1 R_\nu(t) + K_2(t)$ with $K_1 = -(d_\nu + \mu)$ and $K_2(t) = \nu R_u(t)$. Using the duhamel formular, in [35] the solution $R_\nu(t)$ can be given by:

$$R_\nu(t) = e^{\int_0^t -(d_\nu + \mu)d\tau}\left[R_\nu(0) + \int_0^t e^{\int_0^\tau -(d_\nu + \mu)d\tau} \nu R_u(0)e^{(-d_u + \mu + \nu)\tau}d\tau\right].$$

After some transformation, we can easily get

$$R_\nu(t) = e^{-(d_\nu + \mu)t}R_\nu(0) + R_u(0)\nu \frac{1}{d_\nu - d_u - \nu}\left[e^{(-d_u - \mu - \nu)t} - e^{(-d_\nu + \mu)t}\right].$$

Once the expressions of R_u and R_v are found, the system is reduced and can be rewritten as follows:

$$\begin{pmatrix} S'_u \\ S'_v \end{pmatrix} = \begin{pmatrix} \omega S_v - (\mu + v) S_u + d_u R_u + \Lambda \\ v S_u - (\mu + \omega) S_v + d_v R_v \end{pmatrix}. \tag{15}$$

It is possible, by using matrix decomposition properties on this matrix, to obtain:

$$\begin{pmatrix} S'_u \\ S'_v \end{pmatrix} = \begin{pmatrix} -(\mu + v) & \omega \\ v & -(\mu + \omega) \end{pmatrix} \cdot \begin{pmatrix} S_u \\ S_v \end{pmatrix} + \begin{pmatrix} d_u R_u + \Lambda \\ d_v R_v \end{pmatrix}. \tag{16}$$

Let's pose $X = \begin{pmatrix} S_u \\ S_v \end{pmatrix}$; $A = \begin{pmatrix} -(\mu + v) & \omega \\ v & -(\mu + \omega) \end{pmatrix}$ and $B = \begin{pmatrix} d_u R_u + \Lambda \\ d_v R_v \end{pmatrix}$.

The equation (16) is therefore on the form $X'(t) = AX(t) + B(t)$. Using the Duhamel formula, the vector X(t) is given by: $X(t) = e^{tA} X(0) + \int_0^t e^{(t-s)A} B(s) ds$.

A is a diagonalizable matrix with $A = PDP^{-1}$. This will help us compute the exponential expressions in $X(t)$: $e^{tA} = (tP)e^{tD}P^{-1}$ and $e^{A(t-s)} = (t-s)Pe^{(t-s)D}P^{-1}$ with P and D respectively:

$$P = \begin{pmatrix} \frac{\omega - \mu - \sqrt{(\mu-\omega)^2 + 4\mu\omega}}{2v} & \frac{\omega - \mu + \sqrt{(\mu-\omega)^2 + 4\mu\omega}}{2v} \\ 1 & 1 \end{pmatrix}$$

and;

$$D = \begin{pmatrix} \frac{-\omega - \mu - 2v - \sqrt{(\mu-\omega)^2 + 4\mu\omega}}{2} & 0 \\ 0 & \frac{\sqrt{(\mu-\omega)^2 + 4\mu\omega} - \omega - \mu - 2v}{2} \end{pmatrix}.$$

Once, e^{At} and $e^{A(t-s)}$ is replaced in $X(t)$, the solution set S_u, S_v is found. The respective expressions of S_u and S_v (Appendix B.1). With the set (S_u, R_u, S_v, R_v), we can observe that $\lim_{t \to +\infty} S_u(t) = S_u^0(t)$; $\lim_{t \to +\infty} R_u(t) = R_u^0(t) = 0$; $\lim_{t \to +\infty} S_v(t) = S_v^0(t)$ and $\lim_{t \to +\infty} R_v(t) = R_v^0(t) = 0$. Consequently, we have that $p_1 \to p_1^0$ as $t \to \infty$. So $p_1 = p_1^0$ is globally asymptotically stable. Condition 1 is held.

Furthermore, the expression of $\frac{dp_2}{dt}$ is:

$$\frac{dp_2}{dt} = \begin{pmatrix} S_u\lambda_u - (\alpha_e + \nu + \mu)E_u \\ \alpha_e E_u - (\alpha_p + \mu + \nu)I_{P_u} \\ (1-\rho_1)\alpha_p I_{P_u} - (\mu + \nu + \gamma_{a_1+q_{p_1}} + q_{a_1})I_{A_u} \\ \rho_1\alpha_p I_{P_u} - (\mu + \gamma_{s_1} + q_{s_1} + \delta_{s_1})I_{S_u} \\ q_{a_1}I_{A_u} + q_{s_1}I_{S_u} + q_{p_1}I_{P_u} - (\delta_{c_1} + \gamma_{c_1} + \mu)C_u \\ \nu E_u + S_v\lambda_v - (\alpha_e + \mu)E_v \\ \nu I_{P_u} + \alpha_e E_v - (\alpha_p + \mu + q_{p_2})I_{P_v} \\ \nu I_{A_u} + (1-\rho_2)\alpha_p I_{P_v} - (\mu + \gamma_{a_2} + q_{a_2})I_{A_v} \\ \rho_2\alpha_p I_{P_v} - (\mu + \gamma_{s_2} + q_{s_2} + \delta_{s_2})I_{S_v} \\ q_{a_2}I_{A_v} + q_{s_2}I_{S_v} + q_{p_2}I_{P_v} - (\delta_{c_2} + \gamma_{c_2} + \mu)C_v \end{pmatrix}.$$

Now, in determining whether condition 2 would be satisfied, we used the formula $Y_2(p_1, p_2) = B.p_2 - \hat{Y}_2(p_1, p_2)$ and we got:

$$B.p_2 - \hat{Y}_2(p_1, p_2) = \begin{pmatrix} -a_1 & A_{11} & A_{12} & A_{13} & A_{14} & 0 & A_{31} & A_{32} & A_{33} & A_{34} \\ \alpha_e & -a_2 & 0 & 0 & 0 & 0 & 0 & 0 & 0 & 0 \\ 0 & k_5 & -a_3 & 0 & 0 & 0 & 0 & 0 & 0 & 0 \\ 0 & \alpha_p\rho_1 & 0 & -a_4 & 0 & 0 & 0 & 0 & 0 & 0 \\ 0 & q_{p1} & q_{a1} & q_{s1} & -a_5 & 0 & 0 & 0 & 0 & 0 \\ \nu & A_{21} & A_{22} & A_{23} & A_{24} & -a_6 & A_{41} & A_{42} & A_{43} & A_{44} \\ 0 & \nu & 0 & 0 & 0 & \alpha_e & -a_7 & 0 & 0 & 0 \\ 0 & 0 & \nu & 0 & 0 & 0 & k_2 & -a_8 & 0 & 0 \\ 0 & 0 & 0 & 0 & 0 & 0 & \alpha_p\rho_2 & 0 & -a_9 & 0 \\ 0 & 0 & 0 & 0 & 0 & 0 & q_{p2} & q_{a2} & q_{s2} & -a_0 \end{pmatrix} \begin{pmatrix} E_u \\ I_{P_u} \\ I_{A_u} \\ I_{S_u} \\ C_u \\ E_v \\ I_{P_v} \\ I_{A_v} \\ I_{S_v} \\ C_v \end{pmatrix} - \begin{pmatrix} B_1 \\ 0 \\ 0 \\ 0 \\ 0 \\ B_2 \\ 0 \\ 0 \\ 0 \\ 0 \end{pmatrix}.$$

with;

$$B_1 = A_{11}I_{P_u} + A_{12}I_{A_u} + A_{13}I_{S_u} + A_{14}C_u + A_{31}I_{P_v} + A_{32}I_{A_v} + A_{33}I_{S_v} + A_{34}C_v - S_u\lambda_u$$

$$B_2 = A_{21}I_{P_u} + A_{22}I_{A_u} + A_{23}I_{S_u} + A_{24}C_u - A_{41}I_{P_v} + A_{42}I_{A_v} + A_{43}I_{S_v} + A_{44}C_v - S_v\lambda_v.$$

After, replacing the expressions of $A_{11}, A_{12}, A_{13}, A_{14}, A_{31}, A_{32}, A_{33}, A_{34}, A_{21}, A_{22}, A_{23}, A_{24}, A_{41}, A_{42}, A_{43}, A_{44}$ inside B_1 and B_2, we have:

$$B_1 = \left(\frac{S_u^0}{N^0} - \frac{S_u}{N}\right)\left[b_{uu}(1-\psi_u)(I_{P_u}\theta_{p_u} + I_{A_u}\theta_{a_u} + I_{S_u}\theta_{s_u} + C_u\theta_{c_u}) + b_{vu}(1-\psi_v)(I_{P_v}\theta_{p_v} + I_{A_v}\theta_{a_v} + I_{S_v}\theta_{s_v} + C_v\theta_{c_v})\right].$$

$$B_2 = \left(\frac{S_v^0}{N^0} - \frac{S_v}{N}\right)\left[b_{uv}(1-\psi_u)(I_{P_u}\theta_{p_u} + I_{A_u}\theta_{a_u} + I_{S_u}\theta_{s_u} + C_u\theta_{c_u}) + b_{vv}(1-\psi_v)(I_{P_v}\theta_{p_v} + I_{A_v}\theta_{a_v} + I_{S_v}\theta_{s_v} + C_v\theta_{c_v})\right].$$

The matrix B is a matrix with the off-diagonal entries that are all positive. We know that $(S_u/N) \leq (S_u^0/N^0)$, and $(S_v/N) \leq (S_v^0/N^0)$ which implies $\hat{Y}_2(p_1, p_2)$ is positive (having each element greater or equal to zero). As a result, condition 2 is met, demonstrating that the model is globally stable.

3.2.1 *Sensitivity analysis*

The sensitivity analysis studies the variation of the outputs of a model caused by variations in the inputs, and it demonstrates how important each parameter is to disease transmission in terms of positive and negative effects [36]. The sensitivity index, S, of a variable Y with respect to a parameter X is defined by the derivative of Y with respect to X that is:

$$S = \frac{\partial Y}{\partial X}. \tag{17}$$

- The sensitivity of R_c with respect to the vaccination rate v is given by:

$$\frac{\partial R_c}{\partial v} = \frac{\partial R_{c_1}}{\partial v} + \frac{\partial R_{c_2}}{\partial v} + \frac{\partial R_{c_3}}{\partial v} \tag{18}$$

where,

$$\frac{\partial R_{c_1}}{\partial v} = \frac{\partial R_{c_1 Pu}}{\partial v} + \frac{\partial R_{c_1 Au}}{\partial v} + \frac{\partial R_{c_1 Su}}{\partial v} + \frac{\partial R_{c_1 Cu}}{\partial v};$$

with,

$$\frac{\partial R_{c_1 Pu}}{\partial v} = -\frac{\alpha_e b_{uu} \theta_{p_u} (\mu + \omega)(1 - \psi_1)\left(a_1 a_2 + a_2 + a_1(\mu + v + \omega)\right)}{2a_1^2 a_2^2 (\mu + v + \omega)^2};$$

$$\frac{\partial R_{c_1 Au}}{\partial v} = -\frac{\alpha_e \alpha_P b_{uu} \theta_{a_u} (\mu + \omega)(\psi_1 - 1)(\rho_1 - 1)\left(a_1 a_2 a_3 + (\mu + v + \omega)(a_1 a_2 + a_1 a_3 + a_2 a_3)\right)}{2a_1^2 a_2^2 a_3^2 (\mu + v + \omega)^2};$$

$$\frac{\partial R_{c_1 Su}}{\partial v} = -\frac{\alpha_e \alpha_P b_{uu} \rho_1 \theta_{s_u} (\mu + \omega)(1 - \psi_1)\left(a_1 a_2 + (a_1 + a_2)(\mu + v + \omega)\right)}{2a_1^2 a_2^2 a_4 (\mu + v + \omega)^2};$$

$$\frac{\partial R_{c_1 Cu}}{\partial v} = -A\left[a_1 a_2 a_3 + (v + \mu + \omega)(a_1 a_2 + a_1 a_3 + a_2 a_3 - B)\right]$$

where,

$$A = \frac{\alpha_e b_{uu} \theta_{c_u} (1 - \psi_1)(\mu + \omega)\left(a_3 a_4 q_{p1} + a_3 q_{s1} \rho_1 + a_4 \alpha_P q_{a1} (1 - \rho_1)\right)}{2a_1^2 a_2^2 a_3^2 a_4 a_5 (\mu + v + \omega)^2};$$

$$B = \frac{a_1 a_2 a_3 (a_4 q_{p1} + q_{s1} \rho_1)}{a_3 a_4 q_{p1} + a_3 q_{s1} \rho_1 + a_4 \alpha_P q_{a1}(1 - \rho_1)}.$$

Also,

$$\frac{\partial R_{c_2}}{\partial \nu} = \frac{\partial R_{c2P_\nu}}{\partial \nu} + \frac{\partial R_{c2A_\nu}}{\partial \nu} + \frac{\partial R_{c2S_\nu}}{\partial \nu} + \frac{\partial R_{c2C_\nu}}{\partial \nu}$$

with,

$$\frac{\partial R_{c2P_\nu}}{\partial \nu} = \frac{\alpha_e b_{\nu\nu} \theta_{p_\nu} (\mu + \omega)(1 - \psi_2)}{2 a_6 a_7 (\mu + \nu + \omega)^2};$$

$$\frac{\partial R_{c2A_\nu}}{\partial \nu} = \frac{\alpha_e \alpha_P b_{\nu\nu} \theta_{a_\nu} (\mu + \omega)(1 - \psi_2)(1 - \rho_2)}{2 a_6 a_7 a_8 (\mu + \nu + \omega)^2};$$

$$\frac{\partial R_{c2S_\nu}}{\partial \nu} = \frac{\alpha_e \alpha_P b_{\nu\nu} \rho_2 \theta_{s_\nu} (\mu + \omega)(1 - \psi_2)}{2 a_6 a_7 a_9 (\mu + \nu + \omega)^2};$$

$$\frac{\partial R_{c2C_\nu}}{\partial \nu} = \frac{\alpha_e b_{\nu\nu} \theta_{c_\nu} (\mu + \omega)(1 - \psi_2)\left(a_8 \left(a_9 q_{p2} + \alpha_P q_{s2} \rho_2\right) + a_9 \alpha_P q_{a2}(1 - \rho_2)\right)}{2 a_0 a_6 a_7 a_8 a_9 (\mu + \nu + \omega)^2}.$$

Finally,

$$\frac{\partial R_{c_3}}{\partial \nu} = \frac{\partial R_{c_{1\nu}}}{\partial \nu} + \frac{\frac{\partial}{\partial \nu}\left(R_{c_1} - R_{c_2} + R_{c_{1\nu}}\right)\left(R_{c_1} - R_{c_2} + R_{c_{1\nu}}\right) + \frac{2m_1}{m_2} \times \frac{\partial R_{c_1}}{\partial \nu} + 2\frac{\partial R_{c_{1\nu}}}{\partial \nu}}{\sqrt{(R_{c_1} - R_{c_2} + R_{c_{1\nu}})^2 + \frac{4m_1 R_{c_1}}{m_2} + 4R_{c_{1\nu}}}}$$

with,

$$\frac{\partial R_{c_{1\nu}}}{\partial \nu} = \frac{\partial R_{c1A_\nu}}{\partial \nu} + \frac{\partial R_{c1S_\nu}}{\partial \nu} + \frac{\partial R_{c1P_\nu}}{\partial \nu} + \frac{\partial R_{c1C_\nu}}{\partial \nu};$$

where,

$$\frac{\partial R_{c1A_\nu}}{\partial \nu} = C\left[\left(\frac{a_1 a_2 a_3}{\mu + \nu + \omega} + \frac{a_1 a_2 a_3}{\nu} - a_1 a_2 - a_1 a_3 - a_2 a_3\right) + D\right];$$

$$C = \frac{\alpha_e \alpha_P b_{\nu u} \nu \theta_{a_\nu} (1 - \psi_2)(\mu + \omega)(\mu + \nu + \omega)\left(a_3(1 - \rho_2)(a_2 + a_6) + a_6 a_7(1 - \rho_1)\right)}{a_1^2 a_2^2 a_3^2 a_6 a_7 a_8};$$

$$D = \frac{(1 - \rho_2)(a_3 + a_2 + a_6)}{a_3(1 - \rho_2)(a_2 + a_6) + a_6 a_7(1 - \rho_1)};$$

$$\frac{\partial R_{c_1 P v}}{\partial \nu} = \frac{\alpha_e b_{vu} \mu \theta_{p_v}(\mu + \omega)(\psi_2 - 1)\Big(a_1(\mu + \nu + \omega)(\alpha_e + 2\mu - \nu) + I\Big)}{a_1^2 a_2^2 a_6 a_7};$$

$$\frac{\partial R_{c_1 S v}}{\partial \nu} = E\left[a_1 a_2\left(1 + \frac{1}{\nu} + \frac{1}{a_6 + \alpha_P + 2\mu + q_{p1}}\right) - a_1 - a_2\right];$$

$$E = \frac{\alpha_e \alpha_P b_{vu} \nu \rho_2 \theta_{s_v}(1 - \psi_2)(\mu + \omega)(\mu + \nu + \omega)(a_6 + \alpha_P + 2\mu + q_{p1})}{a_1^2 a_2^2 a_6 a_7 a_9};$$

$$\frac{\partial R_{c_1 C v}}{\partial \nu} = F * G\left[a_1 a_2 a_3\left(H + 1 + \frac{1}{\mu + \nu + \omega}\right) - a_1 a_2 - a_1 a_3 - a_2 a_3\right];$$

$$F = \alpha_e b_{vu} \nu \theta_{c_v}(1 - \psi_2)(\mu + \omega)(\mu + \nu + \omega);$$

$$G = \frac{a_3\Big(a_8(a_9 q_{p2} + \alpha_P q_{s2} \rho_2) + a_9 \alpha_P q_{a2}(1 - \rho_2)\Big)(a_6 + \alpha_P + 2\mu + q_{p1}) + J}{a_0 a_1^2 a_2^2 a_3^2 a_6 a_7 a_8 a_9};$$

$$H = \frac{\Big[a_8(a_9 q_{p2} + \alpha_P q_{s2} \rho_2) + a_9 \alpha_P q_{a2}(1 - \rho_2)\Big] K}{a_3(a_6 + \alpha_P + 2\mu + q_{p1}) L + a_6 a_7 a_9 \alpha_P q_{a2}(1 - \psi_1)};$$

$$I = (a_6 + \alpha_P + 2\mu + q_{p1})(\omega - \alpha_e);$$

$$J = (1 - \psi_1) a_6 a_7 a_9 \alpha_P q_{a2};$$

$$K = a_3 + a_8(a_6 + \alpha_P + 2\mu + q_{p1});$$

$$L = a_8(a_9 q_{p2} + \alpha_P q_{s2} \rho_2) + a_9 \alpha_P q_{a2}(1 - \rho_2).$$

- The sensitivity of R_c with respect to the proportion ψ_u is given by:

$$\frac{\partial R_c}{\partial \psi_u} = \frac{\partial R_{c_1}}{\partial \psi_u} + \frac{\partial R_{c_2}}{\partial \psi_u} + \frac{\partial R_{c_3}}{\partial \psi_u} \tag{19}$$

where,

$$\frac{\partial R_{c_1}}{\partial \psi_u} = \frac{\alpha_e b_{uu}(\mu + \omega)\Big(M - \theta_{c_u}\left(a_3 a_4 q_{p1} + a_3 q_{s1}\rho_1 - a_4 \alpha_P q_{a1}(\rho_1 - 1)\right)\Big)}{2 a_2 a_3 a_4 a_5 (a_{66} + \nu)(\mu + \nu + \omega)}$$

with,

$$M = -a_3 a_4 a_5 \theta_{p_u} - a_3 a_5 \alpha_P \rho_1 \theta_{s_u} + a_4 a_5 \alpha_P \theta_{a_u}(\rho_1 - 1);$$

$$\frac{\partial R_{c_2}}{\partial \psi_u} = 0;$$

$$\frac{\partial R_{c_3}}{\partial \psi_u} = \frac{\frac{\partial R_{c_1}}{\partial \psi_u}\left(R_{c_1} - R_{c_2} + R_{c_{1v}} + \frac{2m_1}{m_2}\right)}{\sqrt{(R_{c_1} - R_{c_2} + R_{c_{1v}})^2 + \frac{4m_1 R_{c_1}}{m_2} + 4R_{c_{1v}}}}.$$

- The sensitivity of R_c with respect to the proportion ψ_v is given by:

$$\frac{\partial R_c}{\partial \psi_v} = \frac{\partial R_{c_1}}{\partial \psi_v} + \frac{\partial R_{c_2}}{\partial \psi_v} + \frac{\partial R_{c_3}}{\partial \psi_v} \qquad (20)$$

where,

$$\frac{\partial R_{c_1}}{\partial \psi_v} = 0;$$

$$\frac{\partial R_{c_2}}{\partial \psi_v} = \frac{\alpha_e b_{vv}\nu\Big(N - \theta_{c_v}\left(a_8(a_9 q_{p2} + \alpha_P q_{s2}\rho_2) - a_9 \alpha_P q_{a2}(\rho_2 - 1)\right)\Big)}{2 a_0 a_6 a_7 a_8 a_9 (\mu + \nu + \omega)};$$

$$N = -a_0 a_{88} a_9 \theta_{p_v} - a_0 a_8 \alpha_P \rho_2 \theta_{s_v} + a_0 a_9 \alpha_P \theta_{a_v}(\rho_2 - 1);$$

$$\frac{\partial R_{c_3}}{\partial \psi_v} = \frac{\partial R_{c_{1v}}}{\partial \psi_v} + \frac{\frac{\partial}{\partial \psi_v}\left(R_{c_{1v}} - R_{c_2}\right)\left(R_{c_1} - R_{c_2} + R_{c_{1v}}\right) + 2\frac{\partial R_{c_{1v}}}{\partial \psi_v}}{\sqrt{(R_{c_1} - R_{c_2} + R_{c_{1v}})^2 + \frac{4m1 R_{c_1}}{m_2} + 4R_{c_{1v}}}}$$

with,

$$\frac{\partial R_{c_{1v}}}{\partial \psi_v} = \frac{\partial R_{c_{1Av}}}{\partial \psi_v} + \frac{\partial R_{c_{1Pv}}}{\partial \psi_v} + \frac{\partial R_{c_{1Sv}}}{\partial \psi_v} + \frac{\partial R_{c_{1Cv}}}{\partial \psi_v}$$

where,

$$\frac{\partial R_{c_{1Av}}}{\partial \psi_v} = -\frac{\alpha_e \alpha_P b_{vu} \nu \theta_{a_v} (\mu + \omega) P (\mu + \nu + \omega)}{a_1 a_2 a_3 a_6 a_7 a_8};$$

$$\frac{\partial R_{c_{1Pv}}}{\partial \psi_v} = -\frac{\alpha_e b_{vu} \nu \theta_{p_v} (a_2 + a_6)(\mu + \omega)(\mu + \nu + \omega)}{a_1 a_2 a_6 a_7};$$

$$\frac{\partial R_{c_{1Sv}}}{\partial \psi_v} = -\frac{\alpha_e \alpha_P b_{vu} \nu \rho_2 \theta_{s_v} (\mu + \omega)(\mu + \nu + \omega)(a_{66} + \alpha_P + 2\mu + q_{p1})}{a_1 a_2 a_6 a_7 a_9};$$

$$\frac{\partial R_{c_{1Cv}}}{\partial \psi_v} = -\frac{\alpha_e b_{vu} \nu \theta_{c_v} (\mu + \omega) 0 (\mu + \nu + \omega)}{a_0 a_1 a_2 a_3 a_6 a_7 a_8 a_9};$$

$$O = a_3 \Big(a_8 (a_9 q_{p2} + \alpha_P q_{s2} \rho_2) + a_9 \alpha_P q_{a2} (1 - \rho_2) \Big) (a_6 + \alpha_P + 2\mu + q_{p1}) + Q;$$

$$P = a_3 (1 - \rho_2)(\alpha_e + \alpha_P + 2\mu + \nu + q_{p1}) + a_6 a_7 (1 - \rho_1);$$

$$Q = a_6 a_7 a_9 \alpha_P q_{a2} (1 - \psi_1).$$

- The sensitivity index of R_c with respect to ν and ψ_u

This effect reflects more the reality in the African countries since the control measures were still in place when the vaccination began. This sensitivity represents the gradient of R_c with respect to ν and ψ_u. The gradient of R_c with respect to ν and ψ_u is giving by:

$$J_{(\nu, \psi_u)} R_c = \left(\frac{\partial R_c}{\partial \nu}, \frac{\partial R_c}{\partial \psi_u} \right), \tag{21}$$

where $\frac{\partial R_c}{\partial \nu}$ and $\frac{\partial R_c}{\partial \psi_u}$ are respectively given in the equations (18) and (19).

- The sensitivity index of R_c with respect to ν and ψ_v

This sensitivity index represents the gradient of R_c with respect to ν and ψ_v. The gradient of R_c with respect to ν and ψ_v is giving by:

$$J_{(\nu, \psi_v)} R_c = \left(\frac{\partial R_c}{\partial \nu}, \frac{\partial R_c}{\partial \psi_v} \right), \tag{22}$$

with $\frac{\partial R_c}{\partial \psi_v}$ given in the equation (19).

We also focused on the effect of the variation of transmission parameters linked to the vaccinated people on the control reproduction number. Those parameters are the relative infectiousness of the pre-symptomatic, asymptomatic, symptomatic, and confirmed vaccinated θ_{p_v}, θ_{a_v}, θ_{s_v}, θ_{c_v} as well the infection probabilities, b_{vu} and b_{vv}. Below is the sensitivity index of R_c with respect to the relative infectiousness of the pre-symptomatic, asymptomatic, symptomatic and confirmed vaccinated θ_{p_v}, θ_{a_v}, θ_{s_v}, θ_{c_v} respectively.

- The sensitivity of R_c with respect to the relative infectiousness θ_{p_v} is given by:

$$\frac{\partial R_c}{\partial \theta_{p_v}} = \frac{\partial R_{c_1}}{\partial \theta_{p_v}} + \frac{\partial R_{c_2}}{\partial \theta_{p_v}} + \frac{\partial R_{c_3}}{\partial \theta_{p_v}} \tag{23}$$

where,

$$\frac{\partial R_{c_1}}{\partial \theta_{p_v}} = 0;$$

$$\frac{\partial R_{c_2}}{\partial \theta_{p_v}} = \frac{\alpha_e b_{vv} \nu (1 - \psi_2)}{2a_6 a_7 (\nu + \mu + \omega)};$$

$$\frac{\partial R_{c_3}}{\partial \theta_{p_v}} = \frac{\partial R_{c_{1v}}}{\partial \theta_{p_v}} + \frac{\left(\frac{\partial R_{c_{1v}}}{\partial \theta_{p_v}} - \frac{\partial R_{c_2}}{\partial \theta_{p_v}}\right)\left(R_{c_1} - R_{c_2} + R_{c_{1v}}\right) + 2\frac{\partial R_{c_{1v}}}{\partial \theta_{p_v}}}{\sqrt{(R_{c_1} - R_{c_2} + R_{c_{1v}})^2 + \frac{4m_1 R_{c_1}}{m_2} + 4R_{c_{1v}}}}$$

with,

$$\frac{\partial R_{c_{1v}}}{\partial \theta_{p_v}} = \frac{\alpha_e b_{vu} \nu (1 - \psi_2)(a_2 + a_6)(\mu + \omega)}{a_1 a_2 a_6 a_7}.$$

- The sensitivity of R_c with respect to the relative infectiousness θ_{a_v} is given by:

$$\frac{\partial R_c}{\partial \theta_{a_v}} = \frac{\partial R_{c_1}}{\partial \theta_{a_v}} + \frac{\partial R_{c_2}}{\partial \theta_{a_v}} + \frac{\partial R_{c_3}}{\partial \theta_{a_v}} \tag{24}$$

where,

$$\frac{\partial R_{c_1}}{\partial \theta_{a_v}} = 0;$$

$$\frac{\partial R_{c_2}}{\partial \theta_{a_v}} = \frac{\alpha_e \alpha_P b_{vv} \nu (1 - \psi_2)(1 - \rho_2)}{2a_6 a_7 a_8 (\nu + \mu + \omega)};$$

$$\frac{\partial R_{c_3}}{\partial \theta_{a_v}} = \frac{\partial R_{c_{1v}}}{\partial \theta_{a_v}} + \frac{\left(\frac{\partial R_{c_{1v}}}{\partial \theta_{a_v}} - \frac{\partial R_{c_2}}{\partial \theta_{a_v}}\right)\left(R_{c_1} - R_{c_2} + R_{c_{1v}}\right) + 2\frac{\partial R_{c_{1v}}}{\partial \theta_{a_v}}}{\sqrt{(R_{c_1} - R_{c_2} + R_{c_{1v}})^2 + \frac{4m_1 R_{c_1}}{m_2} + 4R_{c_{1v}}}};$$

with,

$$\frac{\partial R_{c_{1v}}}{\partial \theta_{a_v}} = \frac{\alpha_e \alpha_P b_{vu} \nu \left(1 - \psi_2\right) \left(\mu + \omega\right) \left(a_3 \left(1 - \rho_2\right) \left(a_2 + a_6\right) + a_6 a_7 \left(1 - \rho_1\right)\right) \left(\mu + \nu + \omega\right)}{a_1 a_2 a_3 a_6 a_7 a_8}.$$

- The sensitivity of R_c with respect to the relative infectiousness θ_{s_v} is given by:

$$\frac{\partial R_c}{\partial \theta_{s_v}} = \frac{\partial R_{c_1}}{\partial \theta_{s_v}} + \frac{\partial R_{c_2}}{\partial \theta_{s_v}} + \frac{\partial R_{c_3}}{\partial \theta_{s_v}} \tag{25}$$

where,

$$\frac{\partial R_{c_1}}{\partial \theta_{s_v}} = 0;$$

$$\frac{\partial R_{c_2}}{\partial \theta_{s_v}} = \frac{\alpha_e \alpha_P b_{vv} \nu \rho_2 \left(1 - \psi_2\right)}{2 a_6 a_7 a_9 \left(\nu + \mu + \omega\right)};$$

$$\frac{\partial R_{c_3}}{\partial \theta_{s_v}} = \frac{\partial R_{c_{1v}}}{\partial \theta_{s_v}} + \frac{\left(\frac{\partial R_{c_{1v}}}{\partial \theta_{s_v}} - \frac{\partial R_{c_2}}{\partial \theta_{s_v}}\right)\left(R_{c_1} - R_{c_2} + R_{c_{1v}}\right) + 2\frac{\partial R_{c_{1v}}}{\partial \theta_{s_v}}}{\sqrt{\left(R_{c_1} - R_{c_2} + R_{c_{1v}}\right)^2 + \frac{4 m_1 R_{c_1}}{m_2} + 4 R_{c_{1v}}}}$$

with,

$$\frac{\partial R_{c_{1v}}}{\partial \theta_{s_v}} = \frac{\alpha_e \alpha_P b_{vu} \nu \left(1 - \psi_2\right) \left(\mu + \omega\right) \left(\mu + \nu + \omega\right) \left(a_6 + \alpha_p + 2\mu + q_{p1}\right)}{a_1 a_2 a_6 a_7 a_9}.$$

- The sensitivity of R_c with respect to the relative infectiousness θ_{c_v} is given by:

$$\frac{\partial R_c}{\partial \theta_{c_v}} = \frac{\partial R_{c_1}}{\partial \theta_{c_v}} + \frac{\partial R_{c_2}}{\partial \theta_{c_v}} + \frac{\partial R_{c_3}}{\partial \theta_{c_v}} \tag{26}$$

where,

$$\frac{\partial R_{c_1}}{\partial \theta_{c_v}} = 0;$$

$$\frac{\partial R_{c_2}}{\partial \theta_{c_v}} = \frac{\alpha_e b_{vv} \nu \left(1 - \psi_2\right) \left(a_8 \left(a_9 q_{p2} + \alpha_P q_{s2} \rho_2\right) - a_9 \alpha_P q_{a2} \left(\rho_2 - 1\right)\right)}{2 a_0 a_6 a_7 a_8 a_9 \left(\mu + \nu + \omega\right)};$$

$$\frac{\partial R_{c_3}}{\partial \theta_{c_v}} = \frac{\partial R_{c_{1v}}}{\partial \theta_{c_v}} + \frac{\left(\frac{\partial R_{c_{1v}}}{\partial \theta_{c_v}} - \frac{\partial R_{c_2}}{\partial \theta_{c_v}}\right)\left(R_{c_1} - R_{c_2} + R_{c_{1v}}\right) + 2\frac{\partial R_{c_{1v}}}{\partial \theta_{c_v}}}{\sqrt{(R_{c_1} - R_{c_2} + R_{c_{1v}})^2 + \frac{4m_1 R_{c_1}}{m_2} + 4R_{c_{1v}}}}$$

with;

$$\frac{\partial R_{c_{1v}}}{\partial \theta_{c_v}} = \frac{\alpha_e b_{vu} \nu (S+T)(1-\psi_2)(\mu+\omega)(\mu+\nu+\omega)}{a_0 a_1 a_2 a_3 a_6 a_7 a_8 a_9};$$

$$S = a_3 \left(a_8 \left(a_9 q_{p2} + \alpha_P q_{s2} \rho_2\right) + a_9 \alpha_P q_{a2}(1-\rho_2)\right)\left(a_6 + \alpha_P + 2\mu + q_{p1}\right);$$

$$T = a_6 a_7 a_9 \alpha_P q_{a2}(1-\rho_1).$$

$$E_{\nu R_{c2} P_v} = \frac{\alpha_e \nu b_{vv} \theta_{P_v}(\mu+\omega)(1-\psi_2)}{2a_6 a_7 R_c(\mu+\nu+\omega)^2};$$

$$E_{\nu R_{c2} A_v} = \frac{\alpha_e \nu \alpha_P b_{vv} \theta_{a_v}(\mu+\omega)(1-\psi_2)(1-\rho_2)}{2a_6 a_7 a_8 R_c(\mu+\nu+\omega)^2};$$

$$E_{\nu R_{c2} S_v} = \frac{\alpha_e \nu \alpha_P b_{vv} \rho_2 \theta_{S_v}(\mu+\omega)(1-\psi_2)}{2a_6 a_7 a_9 R_c(\mu+\nu+\omega)^2};$$

$$E_{\nu R_{c2} C_v} = \frac{\alpha_e \nu b_{vv} \theta_{C_v}(\mu+\omega)(1-\psi_2)\left(a_8\left(a_9 q_{p2} + \alpha_P q_{S2} \rho_2\right) + a_9 \alpha_P q_{a2}(1-\rho_2)\right)}{2a_0 a_6 a_7 a_8 a_9 R_c(\mu+\nu+\omega)^2};$$

$$E_{\nu Rc3} = \frac{\nu}{R_c}\left[\frac{\partial R_{c_{1v}}}{\partial \nu} + \frac{\frac{\partial}{\partial \nu}\left(R_{c_1} - R_{c_2} + R_{c_{1v}}\right)\left(R_{c_1} - R_{c_2} + R_{c_{1v}}\right) + \frac{2m_1}{m_2} * \frac{\partial R_{c_1}}{\partial \nu} + 2\frac{\partial R_{c_{1v}}}{\partial \nu}}{\sqrt{\left(R_{c_1} - R_{c_2} + R_{c_{1v}}\right)^2 + \frac{4m_1 R_{c_1}}{m_2} + 4R_{c_{1v}}}}\right].$$

- The elasticity of the control reproduction number with respect to ψ_u is given by:

$$E_{R_c} \mid \psi_u = E_{\psi_u R_{c1}} + E_{\psi_u R_{c2}} + E_{\psi_u R_{c3}} \tag{27}$$

where,

$$E_{\psi_u Rc_1} = \frac{\alpha_e \nu b_{uu}(\mu+\omega)\left(M - \theta_{c_u}\left(a_3 a_4 q_{p1} + a_3 q_{s1} \rho_1 - a_4 \alpha_P q_{a1}(\rho_1 - 1)\right)\right)}{2a_2 a_3 a_4 a_5 R_c(a_{66} + \nu)(\mu+\nu+\omega)};$$

$$E_{\psi_u Rc_2} = 0;$$

$$E_{\psi_u Rc_3} = \left[\frac{\partial R_{c_1}}{\partial \psi_u} \frac{\nu \left(R_{c_1} - R_{c_2} + R_{c_{1v}} + \frac{2m_1}{m_2} \right)}{R_c \sqrt{\left(R_{c_1} - R_{c_2} + R_{c_{1v}} \right)^2 + \frac{4m_1 R_{c_1}}{m_2} + 4R_{c_{1v}}}} \right].$$

- The elasticity of the control reproduction number with respect to ψ_v is given by:

$$E_{R_c} \mid \psi_v = E_{\psi_u R_{c1}} + E_{\psi_u R_{c2}} + E_{\psi_v R_{c3}} \tag{28}$$

where,

$$E_{\psi_v R_{c1}} = 0;$$

$$E_{\psi_v R_{c2}} = \frac{\alpha_e b_{vv} \nu^2 \left(N - \theta_{cv} \left(a_8 \left(a_9 q_{P2} + \alpha_P q_{S2} \rho_2 \right) - a_9 \alpha_P q_{a2} \left(\rho_2 - 1 \right) \right) \right)}{2 a_0 a_6 a_7 a_8 a_9 R_c (\mu + \nu + \omega)};$$

$$E_{\psi_v R_{c3}} = \frac{\nu}{R_c} \left[\frac{\partial R_{c1v}}{\partial \psi_v} + \frac{\frac{\partial}{\partial \psi_v} \left(R_{c1v} - R_{c2} \right) \left(R_{c1} - R_{c2} + R_{c1v} \right) + 2 \frac{\partial R_{c1v}}{\partial \psi_v}}{\sqrt{\left(R_{c1} - R_{c2} + R_{c1v} \right)^2 + \frac{4m1 R_{c1}}{m_2} + 4R_{c1v}}} \right].$$

- The elasticity of the control reproduction number with respect to θ_{p_v} is given by:

$$E_{R_c} \mid \theta_{P_v} = E_{\theta_{P_v} R_{c1}} + E_{\theta_{P_v} R_{c2}} + E_{\theta_{P_v} R_{c3}} \tag{29}$$

where,

$$E_{\theta_{p_v} R_{c1}} = 0;$$

$$E_{\theta_{p_v} R_{c2}} = \frac{\alpha_e b_{vv} \nu^2 (1 - \psi_2)}{2 a_6 a_7 R_c (\nu + \mu + \omega)};$$

$$E_{\theta_{p_v} R_{c3}} = \frac{\nu}{R_c} \left[\frac{\partial R_{c1v}}{\partial \theta_{p_v}} + \frac{\left(\frac{\partial R_{c1v}}{\partial \theta_{p_v}} - \frac{\partial R_{c2}}{\partial \theta_{p_v}} \right) \left(R_{c1} - R_{c2} + R_{c1v} \right) + 2 \frac{\partial R_{c1v}}{\partial \theta_{p_v}}}{\sqrt{\left(R_{c1} - R_{c2} + R_{c1v} \right)^2 + \frac{4m1 R_{c1}}{m_2} + 4R_{c1v}}} \right]$$

- The elasticity of the control reproduction number with respect to θ_{a_v} is given by:

$$E_{R_c} \mid \theta_{a_v} = E_{\theta_{a_v} R_{c1}} + E_{\theta_{a_v} R_{c2}} + E_{\theta_{a_v} R_{c3}} \tag{30}$$

where,

$$E_{\theta_{a_v} R_{c1}} = 0;$$

$$E_{\theta_{a_v} R_{c2}} = \frac{\alpha_e \alpha_P b_{vv} v^2 (1 - \psi_2)(1 - \rho_2)}{2a_6 a_7 a_8 R_c (v + \mu + \omega)};$$

$$E_{\theta_{a_v} R_{c3}} = \frac{v}{R_c} \left[\frac{\partial R_{c1v}}{\partial \theta_{a_v}} + \frac{\left(\frac{\partial R_{c1v}}{\partial \theta_{a_v}} - \frac{\partial R_{c2}}{\partial \theta_{a_v}} \right) \left(R_{c1} - R_{c2} + R_{c1v} \right) + 2 \frac{\partial R_{c1v}}{\partial \theta_{a_v}}}{\sqrt{(R_{c1} - R_{c2} + R_{c1v})^2 + \frac{4m_1 R_{c1}}{m_2} + 4R_{c1v}}} \right].$$

● The elasticity of the control reproduction number with respect to θ_{s_v} is given by:

$$E_{R_c} \mid \theta_{s_v} = E_{\theta_{s_v} R_{c1}} + E_{\theta_{s_v} R_{c2}} + E_{\theta_{s_v} R_{c3}} \tag{31}$$

where,

$$E_{\theta_{s_v} R_{c1}} = 0;$$

$$E_{\theta_{s_v} R_{c2}} = \frac{\alpha_e \alpha_P b_{vv} v^2 \rho_2 (1 - \psi_2)}{2a_6 a_7 a_9 R_c (v + \mu + \omega)};$$

$$E_{\theta_{s_v} R_{c3}} = \frac{v}{R_c} \left[\frac{\partial R_{c1v}}{\partial \theta_{s_v}} + \frac{\left(\frac{\partial R_{c1v}}{\partial \theta_{s_v}} - \frac{\partial R_{c2}}{\partial \theta_{s_v}} \right) \left(R_{c1} - R_{c2} + R_{c1v} \right) + 2 \frac{\partial R_{c1v}}{\partial \theta_{s_v}}}{\sqrt{(R_{c1} - R_{c2} + R_{c1v})^2 + \frac{4m_1 R_{c1}}{m_2} + 4R_{c1v}}} \right].$$

● The elasticity of the control reproduction number with respect to θ_{c_v} is given by:

$$E_{R_c} \mid \theta_{c_v} = E_{\theta_{c_v} R_{c1}} + E_{\theta_{c_v} R_{c2}} + E_{\theta_{c_v} R_{c3}} \tag{32}$$

where,

$$E_{\theta_{c_v} R_{c1}} = 0;$$

$$E_{\theta_{c_v} R_{c2}} = \frac{\alpha_e b_{vv} v^2 (1 - \psi_2) \left(a_8 \left(a_9 q_{p2} + \alpha_P q_{s2} \rho_2 \right) - a_9 \alpha_P q_{a2} \left(\rho_2 - 1 \right) \right)}{2a_0 a_6 a_7 a_8 a_9 R_c (\mu + v + \omega)};$$

$$E_{\theta_{c_v} R_{c3}} = \frac{v}{R_c} \left[\frac{\partial R_{c1v}}{\partial \theta_{c_v}} + \frac{\left(\frac{\partial R_{c1v}}{\partial \theta_{c_v}} - \frac{\partial R_{c2}}{\partial \theta_{c_v}} \right) \left(R_{c1} - R_{c2} + R_{c1v} \right) + 2 \frac{\partial R_{c1v}}{\partial \theta_{c_v}}}{\sqrt{(R_{c1} - R_{c2} + R_{c1v})^2 + \frac{4m_1 R_{c1}}{m_2} + 4R_{c1v}}} \right].$$

- The elasticity of the control reproduction number with respect to b_{vu} is given by:

$$E_{R_c} \mid b_{vu} = E_{b_{vu}R_{c1}} + E_{b_{vu}R_{c2}} + E_{b_{vu}R_{c3}} \tag{33}$$

where,

$$E_{b_{vu}R_{c1}} = 0;$$

$$E_{b_{vu}R_{c2}} = 0;$$

$$E_{b_{vu}R_{c3}} = \frac{v}{R_c} \left[\frac{\partial R_{c1v}}{\partial b_{vu}} + \frac{\frac{\partial R_{c1v}}{\partial b_{vu}} \left(R_{c1} - R_{c2} + R_{c1v} \right) + 2 \frac{\partial R_{c1v}}{\partial b_{vu}}}{\sqrt{(R_{c_1} - R_{c2} + R_{c1v})^2 + \frac{4m_1 R_{c1}}{m_2} + 4R_{c1v}}} \right].$$

- The elasticity of the control reproduction number with respect to b_{vv} is given by:

$$E_{R_c} \mid b_{vv} = E_{b_{vv}R_{c1}} + E_{b_{vv}R_{c2}} + E_{b_{vv}R_{c3}} \tag{34}$$

where,

$$E_{b_{vv}R_{c1}} = 0;$$

$$E_{b_{vv}R_{c2}} = \frac{\alpha_e v \theta_{pv} (1 - \psi_2)}{2a_6 a_7 (\mu + v + \omega)} + \frac{\alpha_e \alpha_p v \rho_2 \theta_{sv} (1 - \psi_2)}{2a_6 a_7 a_9 (\mu + v + \omega)} + \frac{\alpha_e \alpha_P v \theta_{2v} (\psi_2 - 1)(\rho_2 - 1)}{2a_6 a_7 a_8 (\mu + v + \omega)};$$

$$- \frac{\alpha_e v \theta_{4v} (\psi_2 - 1)(a_8 (a_9 q_{p2} + \alpha_P q_{s2} \rho_2) + a_9 \alpha_P q_{a2} (1 - \rho_2))}{2a_0 a_6 a_7 a_8 a_9 (\mu + v + \omega)};$$

$$E_{b_{vv}R_{c3}} = \frac{-\frac{\partial R_{c2}}{\partial b_{vv}} \left(R_{c1} - R_{c2} + R_{c1v} \right)}{\sqrt{(R_{c1} - R_{c2} + R_{c1v})^2 + \frac{4m_1 R_{c1}}{m_2} + 4R_{c1v}}}.$$

3.3 Sensitivity analysis on incidence and mortality

A sensitivity analysis of a dynamical system can yield much qualitative information about how parameters affect the model's compartment dynamics over time. Building upon the results in section 3.2, we specifically examined the effect of the vaccination rate v, the proportions ψ_u and ψ_v that were identified to have the greatest impact on COVID-19 dynamics. It's intriguing to observe how incidence and mortality rates are affected by variations in these parameters is intriguing. The model compartments of interest include confirmed unvaccinated, vaccinated cases (incidence) and unvaccinated, vaccinated deaths (mortality). This technique has been widely used in literature, as evident in several studies [37, 38].

Let $\mathbf{X} = (S_u, E_u, I_{P_u}, I_{A_u}, I_{S_u}, C_u, D_u, R_u, S_v, E_v, I_{P_v}, I_{A_v}, I_{S_v}, C_v, D_v, R_v)$ be the vector of the model states variables; $\mathbf{P} = (v, \psi_u, \psi_v)$ be the vector of the parameters of interest, and the differential equations expressions in the model (3)-(4)

is: $\mathbf{F} = (\dot{S}_u, \dot{E}_u, \dot{I}_{P_u}, \dot{I}_{A_u}, \dot{I}_{S_u}, \dot{C}_u, \dot{D}_u, \dot{R}_u, \dot{S}_v, \dot{E}_v, \dot{I}_{P_v}, \dot{I}_{A_v}, \dot{I}_{S_v}, \dot{C}_v, \dot{D}_v, \dot{R}_v)$. Let's define the sensitivity of the variable's function $V = \frac{\partial X}{\partial P}$. Below is a differential equation system resulting from the total derivative of the function V:

$$\frac{dV}{dt} = \frac{d}{dt}\frac{\partial \mathbf{X}}{\partial \mathbf{P}} = \frac{\partial}{\partial \mathbf{P}}\frac{d\mathbf{X}}{dt} = \frac{\partial \mathbf{F}}{\partial \mathbf{X}}\frac{\partial \mathbf{X}}{\partial \mathbf{P}} + \frac{\partial \mathbf{F}}{\partial \mathbf{P}} = J(\mathbf{X})V + \frac{\partial \mathbf{F}}{\partial \mathbf{P}}. \tag{35}$$

with $J(\mathbf{X})$, a 16×16 Jacobian matrix of the model given as: $\mathbf{J(x)} = [J_{11}\ J_{12}\ J_{13}\ J_{14}]$ with the matrices J_{11}, J_{12}, J_{13} and J_{14} (Appendix B.2).

We can count 16 variables and three parameters, then V is a 16×3 matrix, and $\partial \mathbf{F}/\partial \mathbf{P}$ is a 16×3 matrix.

$$V = \begin{pmatrix} V_{11} & V_{21} & V_{31} & V_{41} & V_{51} & V_{61} & V_{71} & V_{81} & V_{91} & V_{101} & V_{111} & V_{121} & V_{131} & V_{141} & V_{151} & V_{161} \\ V_{12} & V_{22} & V_{32} & V_{42} & V_{52} & V_{62} & V_{72} & V_{82} & V_{92} & V_{102} & V_{112} & V_{122} & V_{132} & V_{142} & V_{152} & V_{162} \\ V_{13} & V_{23} & V_{33} & V_{43} & V_{53} & V_{63} & V_{73} & V_{83} & V_{93} & V_{103} & V_{113} & V_{123} & V_{133} & V_{143} & V_{153} & V_{163} \end{pmatrix}^{\mathrm{T}}.$$

$$V_{11} = \frac{\partial S_u}{\partial v}; \quad V_{21} = \frac{\partial E_u}{\partial v}; \quad V_{31} = \frac{\partial I_{P_u}}{\partial v}; \quad V_{41} = \frac{\partial I_{A_u}}{\partial v}; \quad V_{51} = \frac{\partial I_{S_u}}{\partial v}; \quad V_{61} = \frac{\partial C_u}{\partial v};$$

$$V_{71} = \frac{\partial D_u}{\partial v}; \quad V_{81} = \frac{\partial R_u}{\partial v}; \quad V_{91} = \frac{\partial S_v}{\partial v}; \quad V_{101} = \frac{\partial E_v}{\partial v}; \quad V_{111} = \frac{\partial I_{P_v}}{\partial v}; \quad V_{121} = \frac{\partial I_{A_v}}{\partial v};$$

$$V_{131} = \frac{\partial I_{S_v}}{\partial v}; \quad V_{141} = \frac{\partial C_v}{\partial v}; \quad V_{151} = \frac{\partial D_v}{\partial v}; \quad V_{161} = \frac{\partial R_v}{\partial v}; \quad V_{12} = \frac{\partial S_u}{\partial \psi_u}; \quad V_{22} = \frac{\partial E_u}{\partial \psi_u};$$

$$V_{32} = \frac{\partial I_{P_u}}{\partial \psi_u}; \quad V_{42} = \frac{\partial I_{A_u}}{\partial \psi_u}; \quad V_{52} = \frac{\partial I_{S_u}}{\partial \psi_u}; \quad V_{62} = \frac{\partial C_u}{\partial \psi_u}; \quad V_{72} = \frac{\partial D_u}{\partial \psi_u}; \quad V_{82} = \frac{\partial R_u}{\partial \psi_u};$$

$$V_{92} = \frac{\partial S_v}{\partial \psi_u}; \quad V_{102} = \frac{\partial E_v}{\partial \psi_u}; \quad V_{112} = \frac{\partial I_{P_v}}{\partial \psi_u}; \quad V_{122} = \frac{\partial I_{A_v}}{\partial \psi_u}; \quad V_{132} = \frac{\partial I_{S_v}}{\partial \psi_u}; \quad V_{142} = \frac{\partial C_v}{\partial \psi_u};$$

$$V_{152} = \frac{\partial D_v}{\partial \psi_u}; \quad V_{162} = \frac{\partial R_v}{\partial \psi_u} \quad V_{13} = \frac{\partial S_u}{\partial \psi_v}; \quad V_{23} = \frac{\partial E_u}{\partial \psi_v}; \quad V_{33} = \frac{\partial I_{P_u}}{\partial \psi_v}; \quad V_{43} = \frac{\partial I_{A_u}}{\partial \psi_v};$$

$$V_{53} = \frac{\partial I_{S_u}}{\partial \psi_v}; \quad V_{63} = \frac{\partial C_u}{\partial \psi_v}; \quad V_{73} = \frac{\partial D_u}{\partial \psi_v}; \quad V_{83} = \frac{\partial R_u}{\partial \psi_v}; \quad V_{93} = \frac{\partial S_v}{\partial \psi_v}; \quad V_{103} = \frac{\partial E_v}{\partial \psi_v};$$

$$V_{113} = \frac{\partial I_{P_v}}{\partial \psi_v}; \quad V_{123} = \frac{\partial I_{A_v}}{\partial \psi_v}; \quad V_{133} = \frac{\partial I_{S_v}}{\partial \psi_v}; \quad V_{143} = \frac{\partial C_v}{\partial \psi_v}; \quad V_{153} = \frac{\partial D_v}{\partial \psi_v}; \quad V_{163} = \frac{\partial R_v}{\partial \psi_v}.$$

Regarding, $\frac{\partial \mathbf{F}}{\partial \mathbf{P}}$, we have:

$$\frac{\partial \mathbf{F}}{\partial \mathbf{P}} = \begin{pmatrix} -S_u & \frac{S_u b_{uu}\left(C_u \theta_{c_u}+I_{A_u}\theta_{a_u}+I_{P_u}\theta_{p_u}+I_{S_u}\theta_{s_u}\right)}{N'} & \frac{S_u b_{vu}\left(C_v \theta_{c_v}+I_{A_u}\theta_{a_v}+I_{P_v}\theta_{p_v}+I_{S_v}\theta_{s_v}\right)}{N'} \\[2ex] -E_u & -\frac{S_u b_{uu}\left(C_u \theta_{c_u}+I_{A_u}\theta_{a_u}+I_{P_u}\theta_{p_u}+I_{S_u}\theta_{s_u}\right)}{N'} & -\frac{S_u b_{vu}\left(C_v \theta_{c_v}+I_{A_v}\theta_{a_v}+I_{P_v}\theta_{p_v}+I_{S_v}\theta_{s_v}\right)}{N'} \\[2ex] -I_{P_u} & 0 & 0 \\[1ex] -I_{A_u} & 0 & 0 \\[1ex] 0 & 0 & 0 \\[1ex] 0 & 0 & 0 \\[1ex] 0 & 0 & 0 \\[1ex] -R_u & 0 & 0 \\[1ex] S_u & \frac{S_v b_{uv}\left(C_u \theta_{c_u}+I_{A_u}\theta_{a_u}+I_{P_u}\theta_{p_u}+I_{S_u}\theta_{s_u}\right)}{N'} & \frac{S_v b_{vv}\left(C_v \theta_{c_v}+I_{A_v}\theta_{a_v}+I_{P_v}\theta_{p_v}+I_{S_v}\theta_{s_v}\right)}{N'} \\[2ex] E_u & -\frac{S_v b_{uv}\left(C_u \theta_{c_u}+I_{A_u}\theta_{a_u}+I_{P_u}\theta_{p_u}+I_{S_u}\theta_{s_u}\right)}{N'} & -\frac{S_v b_{vv}\left(C_v \theta_{c_v}+I_{A_v}\theta_{a_v}+I_{P_v}\theta_{p_v}+I_{S_v}\theta_{s_v}\right)}{N'} \\[2ex] I_{P_u} & 0 & 0 \\[1ex] I_{A_u} & 0 & 0 \\[1ex] 0 & 0 & 0 \\[1ex] 0 & 0 & 0 \\[1ex] 0 & 0 & 0 \\[1ex] R_u & 0 & 0 \end{pmatrix}.$$

with $N' = C_u + C_v + D_u + D_v + E_u + E_v + I_{A_u} + I_{A_v} + I_{P_u} + I_{P_v} + I_{S_u} + I_{S_v} + R_u + R_v + S_u + S_v$

3.4 *Applications*
3.4.1 *Model calibration*

In the study, we consider ten African countries, namely: Namibia, South Africa, Rwanda, Lybia, DRC, Nigeria, and Algeria, which were representative of the five (05) regions in Africa. We performed the model calibration to estimate some parameters varying per country. The data for the fitting were obtained from Our World in Data COVID-19 Data respiratory (https://github.com/owid/covid-19-data/tree/master/public/data). This dataset comprises cumulative confirmed COVID-19 cases corresponding to the third wave of the pandemic. The study period differs from country to country, starting from the first day of vaccination to the end of the third wave of the pandemic in each respective country. A summary of the countries with their corresponding study periods is presented in Table 5. To obtain the most accurate, country-specific parameter values and initial conditions, we employed the nonlinear least square technique with the integrated function *fiminsearchbnd* in Matlab (R2021a). We solved, on each training and testing data set, the following optimization problem:

$$\min_{l} f(\boldsymbol{p}) \tag{36}$$

where $f(\boldsymbol{p}) = \sqrt{\frac{1}{n}\sum_{i=1}^{n}(y_{data} - \hat{y}_{pred})^2}$ and l is the set of parameters to estimate. This optimization problem seeks to minimize the Root mean square error between the model-predicted cumulative cases over time and the observed data for each country. In the process of solving the differential equations, we used the following initial conditions: $E_v(0) = I_{P_v}(0) = I_{A_v}(0) = I_{S_v}(0) = C_v(0) = R_v(0) = D_v(0) = 0$. This is because we assumed that the first day of vaccination is a short time to consider vaccinated people going from the susceptible stage to the infected stage. We also assumed the number of susceptible vaccinated individuals $S_v(0)$, being the total number of people vaccinated recipients on the first day of vaccination. This number is specific to each country. The non-varying fixed parameters used in the model fitting process were obtained from the literature, as presented in Table 4.

The remaining country-specific varying parameters, such as recruitment rate, vaccination rate, natural death rate, and force of infection, were computed for the same countries of reference as well as the period of study. The values of the estimated and computed parameters varying per country, as well as the values of the initial conditions, are presented in Table 6.

3.4.1.1 *Recruitment rate*

The recruitment rate Λ considers the birth rate and the net annual immigration. It can be computed using Tovissodé et al. approach [39]. With the average population size during the vaccination period $\overline{N}$, the annual birth rate during the vaccination period b, the net annual immigration ΔI during the vaccination period, the vaccination period in days for each country L, the recruitment rate Λ can be computed as :

$$\Lambda = \frac{b.\overline{N} + \Delta I}{L}, \tag{37}$$

where ΔI is obtained by subtracting the total number of people emigrating from the total number of people immigrating to the country during the vaccination period L. This net quantity is negative if the number of people emigrating is greater than the number of people immigrating, and positive otherwise. The data for the net annual immigration rate for each country was obtained from Worldometer (https://www.worldometers.info/world-population/population-by-country). The annual birth rate was obtained on the latest World Bank data (https://data.worldbank.org/indicator/SP.DYN.CBRT.IN) computed per 1,000 people.

3.4.1.2 *Vaccination rate*

This parameter is computed using the following formula where L is the vaccination time period for each country in days, and p is the proportion of individuals vaccinated with at least one dose of COVID-19 vaccine within that period. Data on the daily vaccination (number of individuals vaccinated with at least one dose) for each selected country was obtained from COVID-19 Data respiratory by Our World in Data (https://github.com/owid/covid-19-data/tree/master/public/data).

$$v = \frac{p}{L} \tag{38}$$

3.4.1.3 *Natural death rate*

Following Sileshi et al. [40], the natural death rate of individuals per day is calculated as the reciprocal of the life expectancy e at the end date (last day of the third wave of the pandemic). It's given by:

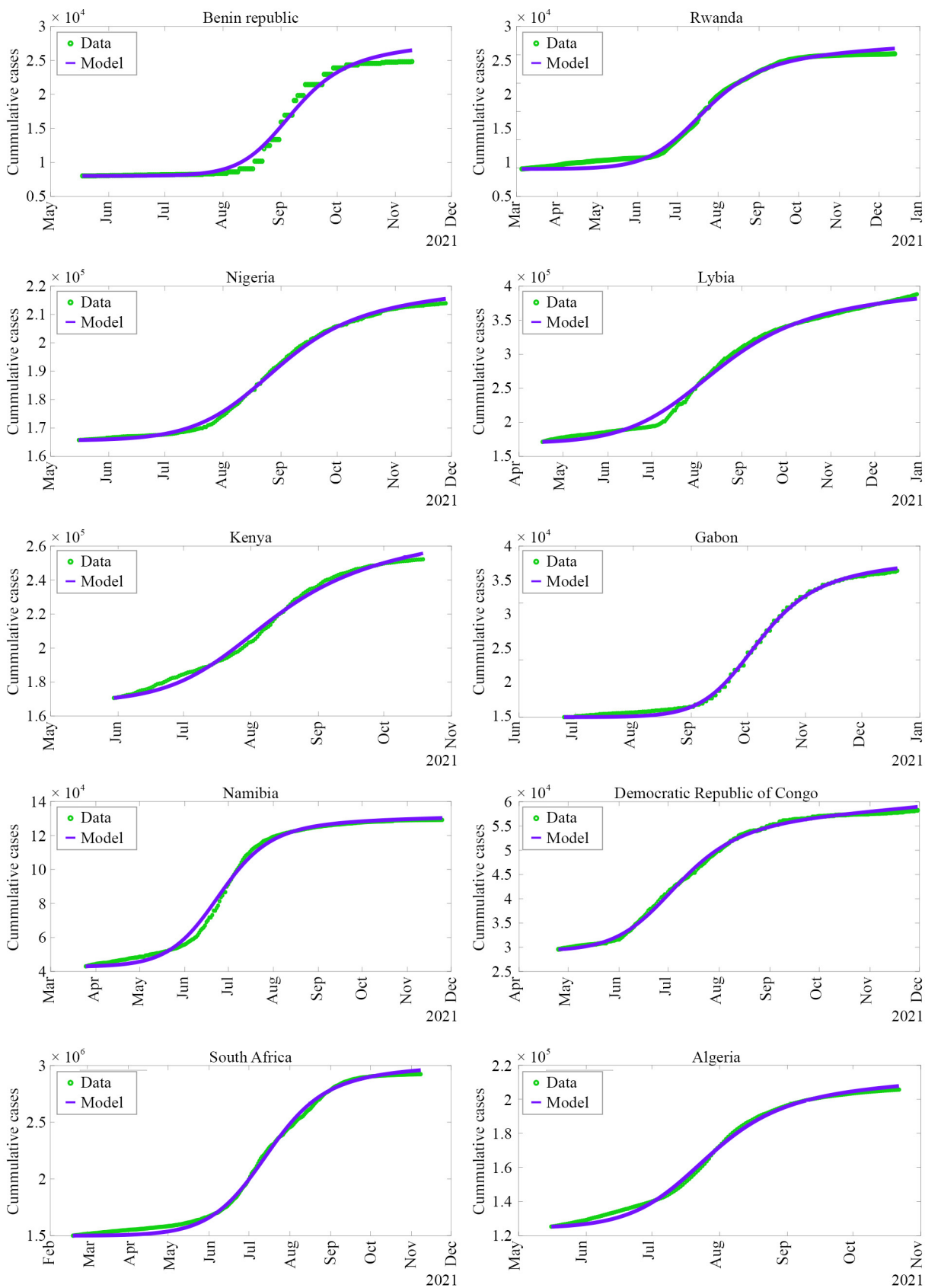$$\mu = \frac{1}{e \times 365}. \tag{39}$$

Figure 2. Model fitting plots using the cumulative confirmed COVID-19 cases in the ten African countries

As illustrated in Figure 2, the model fitting results exhibit close concordance between the cumulative confirmed cases data (green points) and model-predicted cumulative case (blue curve) across the ten examined countries.

3.4.2 *Effect of the vaccination rate, control measures and the transmission parameters on the dynamics of COVID-19 Africa*

This section aims to explore how different parameters of interest affect the control reproduction number R_c and the potential for controlling and eliminating the disease in Africa. For this purpose, we computed the numerical values of the sensitivity and elasticity index using the values of the parameters estimated from the model fitting. The findings from both analyses provide a tool for identifying the key critical model parameters related to vaccination. In line with the sensitivity analysis presented in Table 3, we observed that the parameters have the same index sign across all ten countries. The index linked to the vaccination rate v and the percentage of unvaccinated and vaccinated people following the control measures (ψ_u and ψ_v respectively) have a negative sign, while the parameters related to the virus transmission, such as the infection probabilities (b_{uv}, b_{vv}, b_{vu}) and the relative infectiousness (θ_{p_v}, θ_{a_v}, θ_{s_v} and θ_{c_v}) have a positive sign. This demonstrates that vaccination rate and control measures for the vaccinated and the unvaccinated individuals have a negative effect on the control reproduction number and consequently reduce the number of people infected by the virus. However, the control reproduction number also increases when the infection probabilities increase. In other words, in a situation of high parameter values, a single infected vaccinated or unvaccinated individual will be able to infect more people. A similar interpretation applies to the pre-asymptomatic, asymptomatic, symptomatic, and confirmed vaccinated relative infectiousness. Moreover, we found that the control reproduction number is much more sensitive to the vaccination rate v and the proportion ψ_u of unvaccinated people following the control measures compared to other parameters in every country. This is due to the highest index values corresponding to those two parameters. The sensitivity indices of vaccination rate and control measures are negatives, indicating that all the composites of the gradients in (21) and (22) are negatives. This implies that an increase in the parameters will further decrease the control reproduction number.

Table 3. Sensitivity analysis of the Reproduction number link to the vaccination rate v, the percentage of unvaccinated and vaccinated people following the control measures ψ_u and ψ_v respectively, the infection probabilities b_{vu}, b_{vv}, and the relative infectiousness θ_{p_v}, θ_{a_v}, θ_{s_v} and θ_{c_v}

Countries	Parameters								
	v	ψ_u	ψ_v	b_{vv}	b_{vu}	θ_{p_v}	θ_{a_v}	θ_{s_v}	θ_{c_v}
Namibia	-279.4815	-3.0511	-0.0021	0.0002	0.1908	0.0015	0.0012	0.0003	0.0001
South Africa	-198.0194	-2.5715	-0.0717	0.0056	0.0572	0.0392	0.0380	0.0012	0.0031
Rwanda	-144.5932	-2.2762	-0.1385	0.0306	0.2847	0.1017	0.0934	0.0020	0.0234
Lybia	-241.9733	-2.5289	-0.0362	0.0030	0.1351	0.0354	0.0323	0.0009	0.0079
DRC	-355.8808	-3.2228	-2.5e-04	2.6e-06	0.0198	3.8e-04	3.5e-04	1.9e-05	8.80e-05
Nigeria	-112.7085	-2.8234	-0.1406	0.0172	0.2401	0.0945	0.0970	0.0008	0.0111
Benin	-417.6732	-3.9468	-0.0145	0.0001	0.0124	0.0208	0.0198	0.0001	0.0046
Algeria	-209.2109	-2.7971	-0.1207	0.0122	0.1643	0.1099	0.1170	0.0003	0.0126
Gabon	-402.4471	-3.5067	-0.0099	4.8e-04	0.0688	0.0102	0.0100	3.7e-05	0.0022
Kenya	-298.5017	-2.3849	-0.0339	0.0034	0.0684	0.0439	0.0465	0.0008	0.0085

From a quantitative stand, when all other parameters are held constant, increasing the vaccination rate by 0.01 will decrease the control reproduction number by 2.79 (0.01×279.4815), 1.98, 1.44, 2.41, 3.55, 1.12, 4.17, 2.09, 4.02 and 2.98 in Namibia, South Africa, Rwanda, Lybia, DRC, Nigeria, Benin, Algeria, Gabon, and Kenya respectively. Similarly,
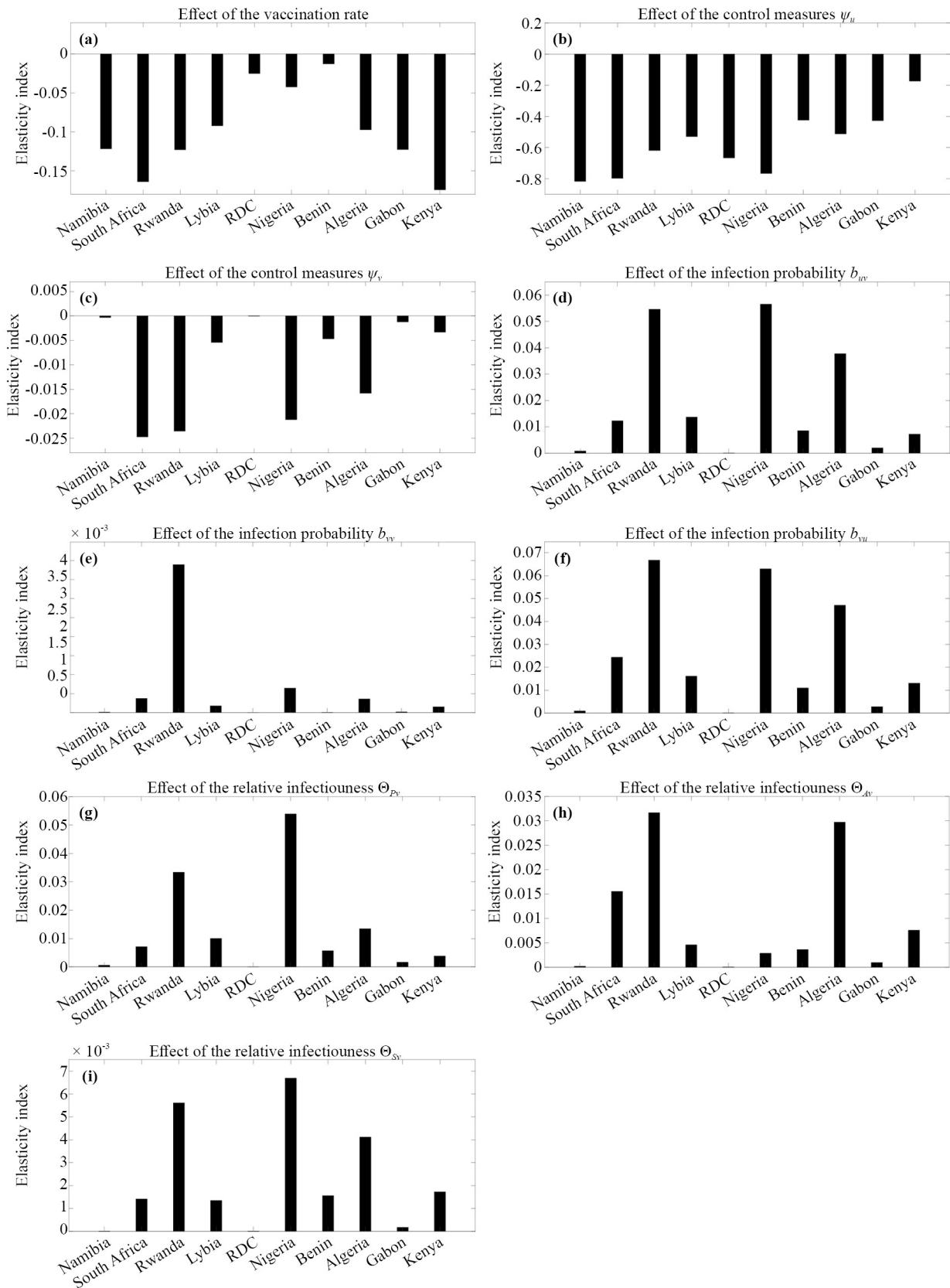
increasing ψ_u by 0.01 will lower the reproduction number by 0.030 (0.01 × 279.4815), 0.025, 0.022, 0.025, 0.032, 0.028, 0.039, 0.027, 0.035 and 0.023 respectively in the same countries.

Interpreting sensitivities can be challenging because parameters are measured in different units. Infection probabilities and proportions ψ_u and ψ_u are probabilities and can only take values between 0 and 1, while vaccination rate and relative infectiousness are not subject to such restrictions. Therefore, comparing their sensitivity index may be difficult. This is where elasticity comes into play. The elasticity analysis performed in Figure 3 presents the results of the elasticity analysis, which estimates the effect of a proportional change in parameters on the transmission dynamics of COVID-19. A comprehensive analysis of the results presented in Figure 3 revealed that the parameter ψ_u has the most significant impact on the R_c in all ten African countries, with values ranging from -0.8174 to -0.1741. When the proportion of people unvaccinated adhering to the control measures decreases by 10%, the control reproduction number increases by 8.174% in Namibia, 7.980% in South Africa, 6.195% in Rwanda, 5.2% in Lybia, 6.66% in DRC, 7.66% in Nigeria, 4.23% in Benin, 5.12% in Algeria, 4.27% in Gabon and 1.74% in Kenya. A larger unvaccinated population following the control measures causes more infected cases. Thus, isolating that population and constraining them to wash their hands, follow social distancing, or wear a mask is one of the most effective measures to reduce the virus transmission, particularly in Namibia, where the elasticity index is the highest.

The findings from Figure 3 further reveal that vaccination rate is the second most influential parameter on the control reproduction number in the studied countries. When the vaccination rate increases by 10%, the control reproduction number decreases by 1.217% in Namibia, 1.640% in South Africa, 1.230% in Rwanda, 0.92% in Lybia, 0.251% in DRC, 0.424% in Nigeria, 0.127% in Benin, 0.973 % in Algeria, 1.226% in Gabon and 1.74% in Kenya. An effective way to slow down the outbreak will be controlling the vaccination rate of the susceptible, exposed, pre-asymptomatic, and asymptomatic individuals. A mass vaccination campaign targeting individuals in these classes could play an important role in controlling the outbreak.

In contrast, results in Figure 3 show that the proportion of vaccinated people, ψ_v, has a lesser effect on the control reproduction number than the proportion of unvaccinated people. A 10% decrease in ψ_v results in a minimal increase of 1.217% in R_c in Namibia, 1.640% in South Africa, 1.230% in Rwanda, 0.92% in Libya, 0.251% in DRC, 0.424% in Nigeria, 0.127% in Benin, 0.973% in Algeria, 1.226% in Gabon, and 1.74% in Kenya. Even though decreasing this parameter does have a negative effect, it is not as severe as that of the proportion of the unvaccinated. This means that even if few vaccinated people adhere to control measures, it won't increase transmission as much as when unvaccinated people do not follow control measures. Therefore, a vaccination campaign plays a crucial role in reducing the risk of disease transmission by unvaccinated individuals who don't follow control measures. Additionally, from this comparison, improving the control measures on the unvaccinated more than the vaccinated is of utmost importance to control and prevent further outbreaks of the pandemic.

Compared to the previous parameters, it can be observed that the control reproduction number increases as the remaining parameters increase, and the effect is less sensitive. A 10% increase in the probability b_{vv} results in a 1.160e-04% increase in control reproductions in Namibia, 3.73e-03% in South Africa, 0.039% in Rwanda, 1.7864e-03% in Lybia, 8.43e-07% in DRC, 6.44e-03% in Nigeria, 7.02e-05% in Benin, 3.59e-03 % in Algeria, 1.97e-04% in Gabon, and 1.53e-03% in Kenya while a 10% increase in the probability b_{vu} generate an increase of 8.1704e-03% in Namibia, 0.123% in South Africa, 0.546% in Rwanda, 0.137% in Lybia, 8.0965e-04% in DRC, 0.566% in Nigeria, 0.085% in Benin, 0.377% in Algeria, 0.020% in Gabon, and 0.072% in Kenya. These results show that vaccinated individuals are more likely to infect unvaccinated individuals than themselves, suggesting that vaccination reduces the chances of getting infected with the disease in the overall population.
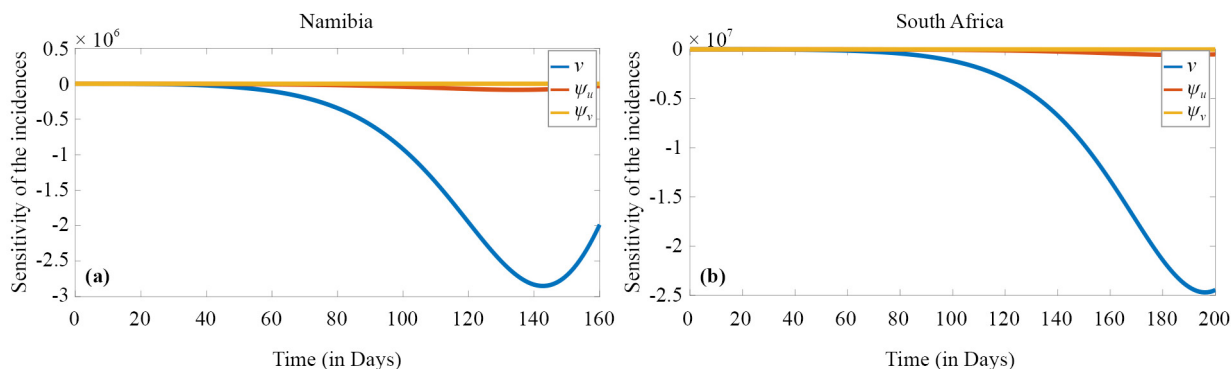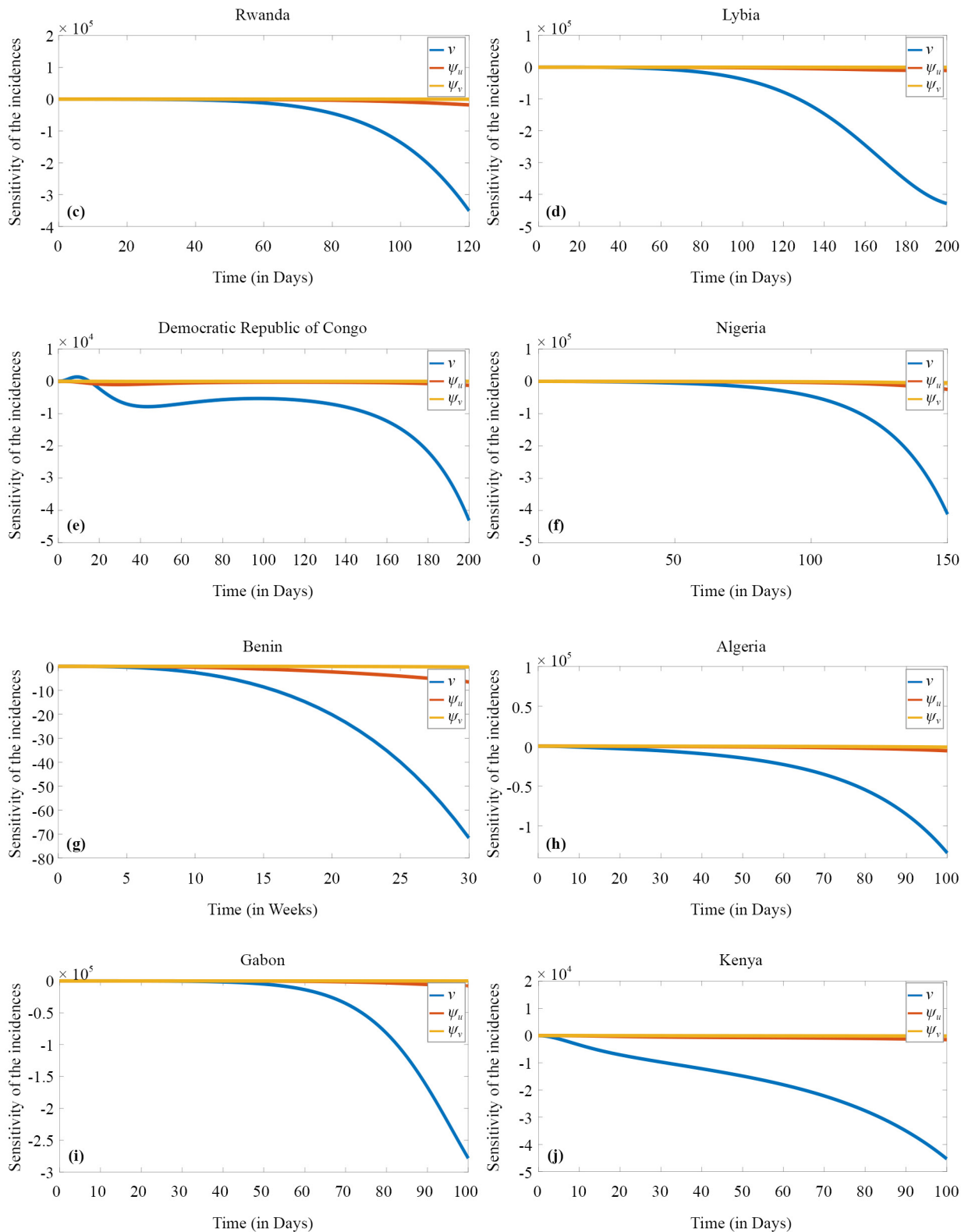
Figure 3. Elasticity analysis of the reproduction number with respect to: (a) the vaccination rate ν, (b) the proportion of unvaccinated people following the control measures ψ_u, (c) the proportion of unvaccinated people following the control measures ψ_v, (d) the infection probability b_{uv}, (e) the infection probability b_{vu}, (f) the relative infectiousness θ_{p_v}, (g) the relative infectiousness θ_{a_v}, (h) the relative infectiousness θ_{s_v} and (i) the relative infectiousness θ_{c_v}

Regarding the remaining parameters, that is, the relative infectiousness θ_{p_v}, θ_{a_v}, θ_{s_v} and θ_{c_v} of the vaccinated, the elasticity index demonstrates negligible significance when compared to the previous parameters. The findings have shown that a 10% increase in these parameters does not substantially increase the control reproduction number across countries. This indicates that pre-symptomatic, asymptomatic, symptomatic, and confirmed vaccinated individuals can infect less, especially the confirmed and the symptomatic communities, whose elasticity values vary from 9.72e-06 to 0.0067 and 3.03e-06 to 6.36e-04, respectively, among the countries, thus their role in disease transmission is not essential. The results align with the results of the initial sensitivity analysis conducted.
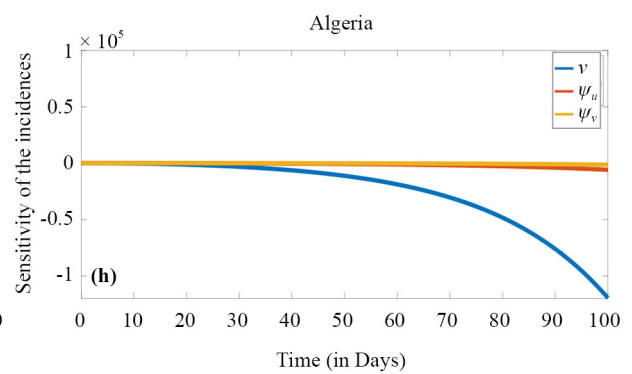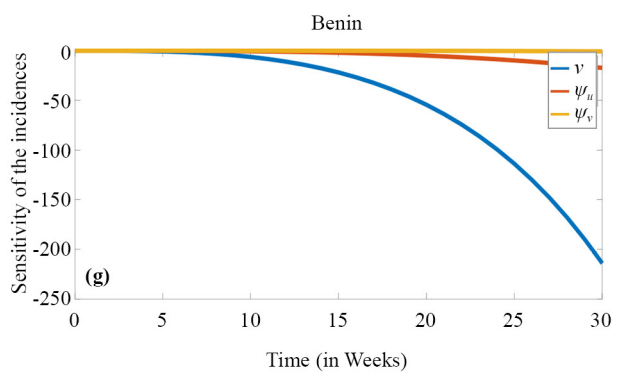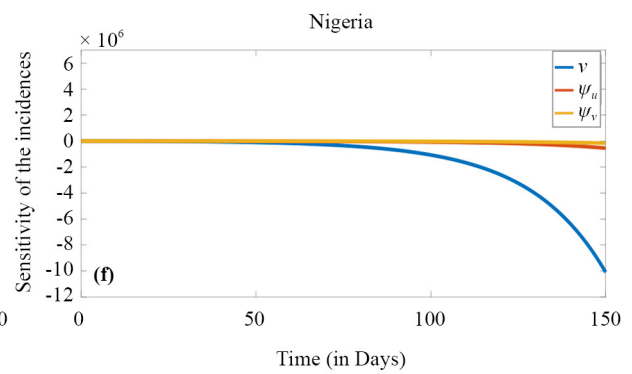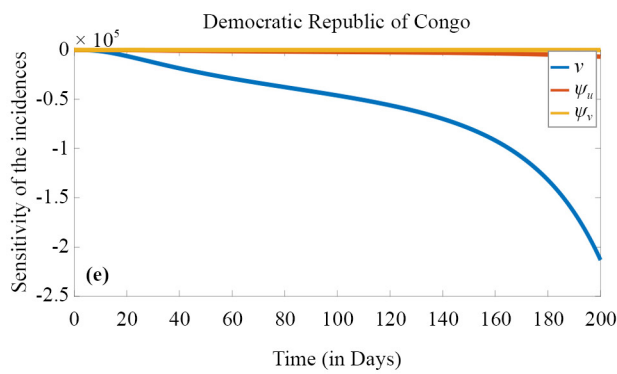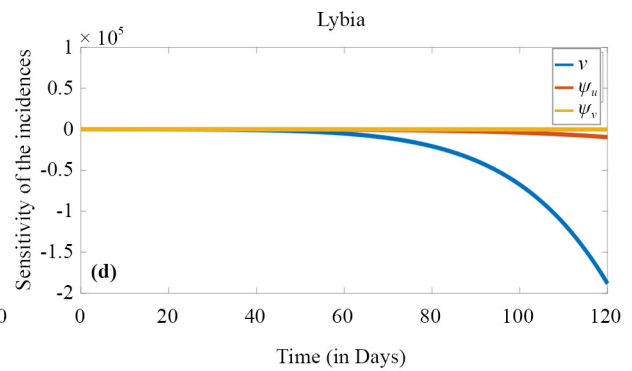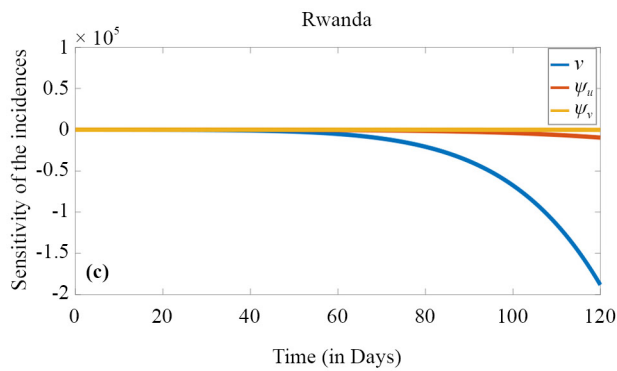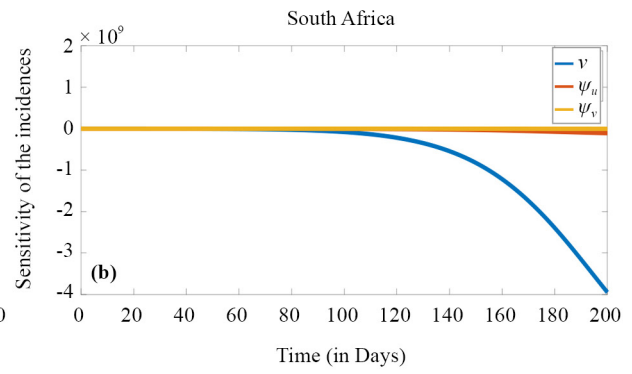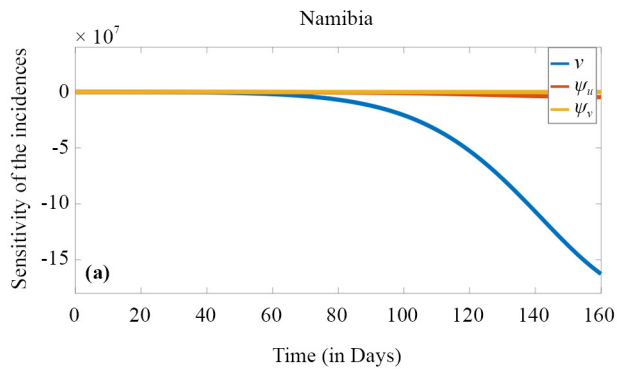
3.4.3 *Effect of vaccination rate and control measures on the incidences and mortality in Africa*
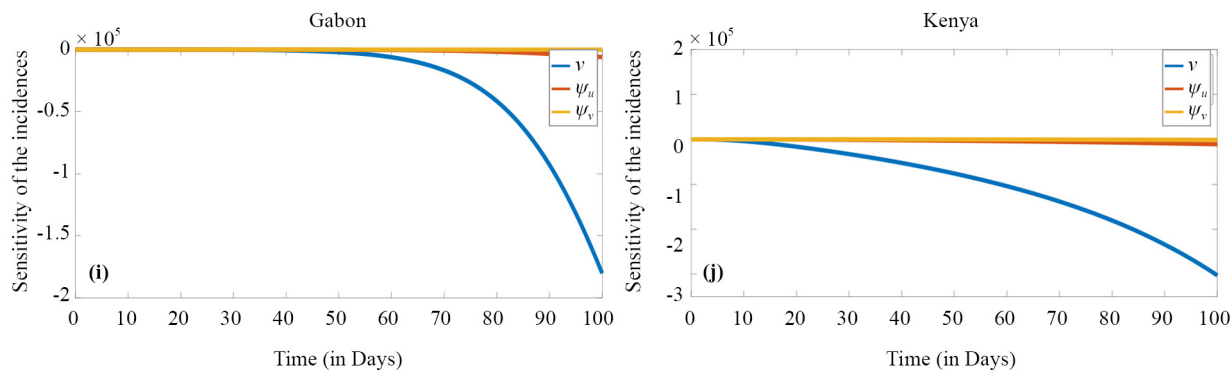
We conducted sensitivity simulations by numerically solving the differential system equation in (35) using ODE45 in Matlab with the initial values $V_0 = 0_{16 \times 3}$ (16×3 zeroes matrix). Tables 4 and 6 present the parameter values for the simulation. Since our main focus was the incidences and mortality, we plotted the matrix elements [V61 + V141]; [V62 + V142]; [V63 + V143], respectively related to the vaccination rate v, the proportions ψ_u, and ψ_v. These elements correspond to both the vaccinated and unvaccinated confirmed case compartments. Additionally, we plotted the elements [V71 + V151] (v), [V72+V152] (ψ_u) and [V73 + V153] (ψ_v) for the deaths cases. The results are presented per country in Figure 4 for the incidences and Figure 5 for the mortality. At any given time, we can observe the effect of each parameter's changes on each variable. The positivity of the sensitivity values indicates that an increase in the parameter leads to a higher value of the variable. Conversely, a negative sensitivity value indicates a negative relationship between the parameter and the variable. A value zero of the sensitivity means that changes in the parameter's value do not affect the variable. Globally, the plots show that the sensitivity values start from zero and decrease over time for each of the three parameters, whether for incidences or mortality. This is the case in all countries. It means that the parameters v, ψ_u, and ψ_v affect the incidences and mortality negatively. Consequently, there are more susceptible, exposed, pre-symptomatic, or recovered people vaccinated, and significantly fewer incidences and dead people of COVID-19 in Africa. Similarly, with a higher proportion of adherence to the control measures, the number of confirmed cases and deaths was reduced. Furthermore, of the three parameters, the one that has the most influence on changing incidences and mortality is the vaccination rate. These results confirm that vaccination associated with high adherence to control measures reduces the incidence and mortality of COVID-19 in Africa.

Figure 4. Time-dependent sensitivity analysis of the incidences with respect to the vaccination rate v, the proportion of unvaccinated people and vaccinated people following the control measures ψ_u and ψ_v. Panels (a-j) are, respectively, for the cases of Namibia, South Africa, Rwanda, Lybia, the Democratic Republic of Congo, Nigeria, Benin, Algeria, Gabon, and Kenya

Figure 5. Time-dependent sensitivity analysis of the mortality with respect to the vaccination rate v, the proportion of unvaccinated people and vaccinated people following the control measures ψ_u and ψ_v. Panels (a-j) are, respectively, for the cases of Namibia, South Africa, Rwanda, Lybia, the Democratic Republic of Congo, Nigeria, Benin, Algeria, Gabon, and Kenya

4. Discussion

A big challenge in epidemiology is understanding how infectious diseases spread. This is usually investigated through modeling [41, 42]. Using models, public health decision-makers can make the most efficient use of resources and reduce epidemic severity [43]. The following paper proposes a compartmental model of the COVID-19 outbreak constituted of susceptible, exposed, pre-symptomatically infectious, asymptomatically infectious, symptomatically infectious, confirmed cases, death cases, and recovered populations. We analyzed the mathematical model analytically and observed that model solutions remained positive and bounded. Additionally, using the Castillo Chevez method, we have demonstrated that the disease-free equilibrium is globally stable when the control reproduction number R_c is less than one unit. The model was calibrated using COVID-19 cumulative case data for each country for the third wave of the COVID-19 pandemic. We then derived the sensitivity and elasticity expressions to assess the effect of the vaccination rate, the control measures, the infection probabilities, and the relative infectiousness on the control reproduction number.

According to the results, vaccination rates and unvaccinated people's compliance with control measures significantly impacted the control reproduction number. Similarly, combining control strategies with a high percentage of vaccinated people will effectively slow the COVID-19 virus spreading in Africa. Based on the parameters with the highest effect on the COVID-19 transmission dynamics, we examined the numerical sensitivity analysis of the incidences and mortality. The results were presented regarding the temporal dynamics sensitivity of the confirmed and death cases, illustrating that the vaccination rate significantly reduces the number of confirmed and death cases as established in the study [44]. The results also highlight that the parameter representing the control measures for the unvaccinated diminishes the confirmed cases and fatalities as time progresses. Consequently, when vaccination rates and the proportion of unvaccinated people wearing masks, washing hands, and following social distancing are low, containing the virus spread can not be effective. To summarize, maintaining a high vaccination rate and control measures for unvaccinated people are essential to eliminate the COVID-19 virus.

We incorporated heterogeneity of transmission in the model by dividing the population into two groups: those who are vaccinated and those who are not. This might not be sufficient to capture the actual dynamics of the transmission of COVID-19 in the population and could be addressed with other modeling approaches, such as agent-based modeling [45]. Such models, however, introduce many open parameters that need to be estimated using data from different sources (e.g., localization data) that may not have been available during the epidemic, particularly in Africa. In light of this, we opted for a compartmental model that was less complex but with extensions increasing the accuracy of the model by adding compartments and parameters that could be calculated using the available data. Also, we assume that individuals who show severe symptoms and those from confirmed cases cannot be vaccinated, as considered in this study [46].

Our model provides estimates of control reproduction numbers (R_c) for ten African nations that account for vaccination effects including Namibia ($R_c = 1.713$), South Africa ($R_c = 1.500$), Nigeria ($R_c = 1.599$), Libya ($R_c = 1.432$),

DR Congo ($R_c = 1.682$), Rwanda ($R_c = 1.806$), Algeria ($R_c = 1.902$), Kenya ($R_c = 1.911$), Benin ($R_c = 2.79$) and Gabon ($R_c = 2.37$). South Africa and Algeria exhibit the largest relative drops from an R_0 of 3.1 and 3.6 to a R_c of 1.50 and 1.90, respectively, representing over a 50% reduction. In assessing our modeling approach's efficiency, comparative analyses revealed close concordance between our R_c estimations and those from prior modeling studies utilizing different techniques utilizing techniques such as individual-based stochastic simulations [47].

Also, as an example, the early endemic South-Africa-based model results by Rabiu Musa and Iyaniwura Sarafa [48] that considers the waning of both vaccine-induced immunity and post-recovery immunity estimated R_c up to 1.23 while maintaining a vaccine waning rate of 0.5. This value is close to what our model estimated. The precise approximation of the R_c for each nation demonstrates our model's efficiency in capturing heterogeneous transmission patterns. For instance, our model reliably predicted Rwanda's lower R_c of 1.806, aligning with evidence of effective control policies from past research [49]. Whereas higher R_c valuations for Algeria (1.902) and Kenya (1.911) accurately reflected relaxed restrictions and elevated disease spread. By generating country-specific R_c estimates closely mirroring those derived via different modeling techniques, our approach displayed its ability to reliably simulate region-particular transmission dynamics.

Despite the size of the model, which has sixteen state variables and forty parameters, we fail to consider every factor to represent the dynamics of COVID-19 in the face of vaccination. We assume that both asymptomatic and symptomatic infectious cases move into the confirmed class, although this may not be true in all countries. For example, this study from South Africa [50] didn't include a route for asymptomatic individuals to move into the confirmed class. Also, we did not include multiple doses that an individual may have received regarding the fact that most of the COVID-19 vaccines available today need more than one dose to provide adequate protection. Instead, we stated that the vaccinated populations had been vaccinated at least once.

A possible future approach is expanding the model to include precise infection or immune decline cycles. There will be sixteen compartments of our current model in each cycle. Individuals who lose their natural immunity and vaccine immunity will move to the susceptible unvaccinated compartment of the next cycle instead of the susceptible unvaccinated compartment of their current cycle, as in our current model. One advantageous aspect of formulating the model in such a structure is that the number of individuals infected during each infection cycle can be easily tracked. In addition, at this time, variants of the SARS-COV-2 virus had emerged in many African countries. Defining different cycles of infection can be interpreted as susceptibility to other variants of COVID-19.

Another limitation in our model pertains to the assumption of a homogeneous mixed population. In fact, contact rates and mixing patterns may exhibit variations among individuals based on age and activity level. Stratifying the population by age is also an interesting approach to investigate since young people are not allowed to get vaccinated. Despite these aforementioned limitations, the employed modeling approach has provided valuable insights into understanding the dynamics of COVID-19 in the face of vaccination, as well as some plausible recommendations on crucial factors to consider in curtailing the COVID-19 virus.

5. Conclusion and perspectives

The COVID-19 pandemic has emerged as an immensely destructive disease that has profoundly impacted global populations, and Africa has not been excluded. Businesses closed, schools closed, travel restrictions in place, and regulations on the limitation of social interaction, among other containment measures. In this research study, we have developed an expanded SEIR mathematical model to incorporate the vaccination program in the context of Africa. We performed extensive analytical analyses by checking the positiveness and boundedness of the model solutions. The global stability analysis for the disease-free equilibrium performed using the Castillo-Chavez method revealed that the model is globally stable when the control reproduction number is less than 1. Furthermore, both control and basic reproduction numbers have been derived. We fitted the model using cumulative case data resulting from the third wave of the pandemic. The study also encompassed numerical sensitivity and elasticity analyses to identify the influential parameters that should be targeted to reduce the control reproduction number, as well as incidences and mortality rates. Interestingly, it was

observed that the transmission rate from vaccinated individuals exhibited a minor effect on the control reproduction number. However, the vaccination rate and the proportion of unvaccinated individuals adhering to control measures were found to have a substantial influence. Simulation results revealed that the vaccination rate and the percentage of unvaccinated individuals following control measures were highly effective in reducing the number of COVID-19 confirmed cases and fatalities. To effectively mitigate the transmission dynamics of the pandemic and curb the incidence and mortality rates in Africa, it is imperative to achieve higher vaccination rates among pre-symptomatic, exposed, or recovered individuals. Furthermore, a crucial aspect is to ensure a greater proportion of unvaccinated individuals adhering to control measures compared to vaccinated individuals. It is worth noting that the pandemic continues to spread across the continent, underscoring the significance of the findings from this study as valuable inputs for policymaking by African governments. As long as the pandemic persists, it is of utmost importance to implement compulsory mass vaccination campaigns and enforce personal protective measures to effectively mitigate the devastating effects of the COVID-19 pandemic and safeguard the well-being of African nations. We are investigating possibilities to optimize the model to fit the COVID-19 evolution in Africa with more accurate methods. Future projects in this field may explore the integration of behavioral modeling to understand how pandemic dynamics respond to public behavior changes combined with vaccination campaigns.

Acknowledgement

Conflict of interest

The authors declare no conflicts of interest. The funders had no role in the design of the study; in the collection, analyses, or interpretation of data; in the writing of the manuscript; or in the decision to publish the results.

References

[1] Yavuz M, Coşar FÖ, Günay F, Özdemir FN. A new mathematical modeling of the COVID-19 pandemic including the vaccination campaign. *Open Journal of Modelling and Simulation*. 2021; 9(3): 299-321.

[2] WHO. *COVID-19 overview*. Geneva, Switzerland: World Health Organization; 2023. Available from: https://www.who.int/europe/emergencies/situations/covid-19 [Accessed 3rd February 2023].

[3] WHO. *COVID-19 overview emergencies*. World Health Organization; 2023. Available from: https://www.who.int/emergencies/diseases/novel-coronavirus-2019/situation-reports [Accessed 3rd Feb 2023].

[4] WHO Africa. *Cumulative cases and deaths*. World Health Organization; 2023. Available from: https://who.maps.arcgis.com/apps/dashboards/0c9b3a8b68d0437a8cf28581e9c063a9 [Accessed 4th Jan 2023].

[5] Duhon J, Bragazzi N, Kong JD. The impact of non-pharmaceutical interventions, demographic, social, and climatic factors on the initial growth rate of COVID-19: A cross-country study. *Science of the Total Environment*. 2021; 760: 144325.

[6] Bwire G, Ario AR, Eyu P, Ocom F, Wamala JF, Kusi KA, et al. The COVID-19 pandemic in the African continent. *BMC Medicine*. 2022; 20(1): 1-23.

[7] Rémy V, Largeron N, Quilici S, Carroll S. The economic value of vaccination: Why prevention is wealth. *Journal of Market Access & Health Policy*. 2015; 3(1): 29284.

[8] Brauer F, Castillo-Chavez C, Feng Z. *Mathematical models in epidemiology, vol. 32*. Springer; 2019.

[9] Samui P, Mondal J, Khajanchi S. A mathematical model for COVID-19 transmission dynamics with a case study of India. *Chaos, Solitons & Fractals*. 2020; 140: 110173.

[10] Garba SM, Lubuma JMS, Tsanou B. Modeling the transmission dynamics of the COVID-19 Pandemic in South Africa. *Mathematical Biosciences*. 2020; 328: 108441.

[11] Photphanloet C, Shuaib S, Ritraksa S, Riyapan P, Intarasit A. *A mathematical model to assess COVID-19 vaccination in Thailand*. Authorea Preprints; 2022. Available from: https://doi.org/10.22541/au.164352416.63424157/v1.

[12] Choi Y, Kim JS, Kim JE, Choi H, Lee CH. Vaccination prioritization strategies for COVID-19 in Korea: A mathematical modeling approach. *International Journal of Environmental Research and Public Health*. 2021; 18(8): 4240.

[13] Li M, Zu J, Zhang Y, Ma L, Shen M, Li Z, et al. COVID-19 epidemic in New York City: Development of an age group-specific mathematical model to predict the outcome of various vaccination strategies. *Virology Journal*. 2022; 19(1): 1-13.

[14] Dos Reis EV, Savi MA. A dynamical map to describe COVID-19 epidemics. *The European Physical Journal Special Topics*. 2022; 231(5): 893-904.

[15] Love J, Keegan LT, Angulo FJ, McLaughlin JM, Shea KM, Swerdlow DL, et al. Continued need for non-pharmaceutical interventions after COVID-19 vaccination in long-term-care facilities. *Scientific Reports*. 2021; 11(1): 1-5.

[16] Abboubakar H, Racke R. *Mathematical modeling of the Coronavirus (Covid-19) transmission dynamics using classical and fractional derivatives*. University of Constance; 2022. Available from: http://nbn-resolving.de/urn:nbn:de:bsz:352-2-128ngycit58bu5.

[17] Sivashankar M, Sabarinathan S, Govindan V, Fernandez-Gamiz U, Noeiaghdam S. Stability analysis of COVID-19 outbreak using Caputo-Fabrizio fractional differential equation. *AIMS Mathematics*. 2023; 8(2): 2720-2735. Available from: https://doi.org/10.3934/math.2023143.

[18] Kumar P, Rangaig NA, Abboubakar H, Kumar A, Manickam A. Prediction studies of the epidemic peak of coronavirus disease in Japan: From Caputo derivatives to Atangana-Baleanu derivatives. *International Journal of Modeling, Simulation, and Scientific Computing*. 2022; 13(1): 2250012.

[19] Hess S, Lancsar E, Mariel P, Meyerhoff J, Song F, van den Broek-Altenburg E, et al. The path towards herd immunity: Predicting COVID-19 vaccination uptake through results from a stated choice study across six continents. *Social Science & Medicine*. 2022; 298: 114800.

[20] Adane M, Ademas A, Kloos H. Knowledge, attitudes, and perceptions of COVID-19 vaccine and refusal to receive COVID-19 vaccine among healthcare workers in northeastern Ethiopia. *BMC Public Health*. 2022; 22(1): 1-14.

[21] Hlongwa M, Afolabi A, Dzinamarira T. Hesitancy towards a COVID-19 vaccine in selected countries in Africa: Causes, effects and strategies for improving COVID-19 vaccine uptake. *Global Biosecurity*. 2022; 3(1): 1-5. Available from: https://doi.org/10.31646/gbio.130.

[22] Adeleke O, Adegboro J, Olofintuyi O, Ayenigbara I, Aina S, Fadero E, et al. Factors of predicting the acceptance of the COVID-19 vaccine in West Africa (a cross-sectional study in Nigeria). *Journal of Applied Health Sciences*. 2022; 8(1): 5-13.

[23] Thirthar AA, Abboubakar H, Khan A, Abdeljawad T. Mathematical modeling of the COVID-19 epidemic with fear impact. *AIMS Math*. 2023; 8(3): 6447-6465.

[24] Honfo SH, Taboe HB, Kakaï RG. Modeling COVID-19 dynamics in the sixteen West African countries. *Scientific African*. 2022; 18: e01408.

[25] Yedomonhan E, Tovissodé CF, Kakaï RG. Modeling the effects of Prophylactic behaviors on the spread of SARS-CoV-2 in West Africa. *Mathematical Biosciences and Engineering*. 2023; 20(7): 12955-12989.

[26] Montcho Y, Nalwanga R, Azokpota P, Doumatè JT, Lokonon BE, Salako VK, et al. Assessing the impact of vaccination on the dynamics of COVID-19 in Africa: A mathematical modeling study. *Vaccines*. 2023; 11(4): 857.

[27] Gumel AB, Iboi EA, Ngonghala CN, Ngwa GA. Towards achieving a vaccine-derived herd immunity threshold for COVID-19 in the US. *Frontiers in Public Health*. 2021; 9: 1-30. Available from: https://doi.org/10.1101/-2020.12.11.20247916.

[28] Wang X, Fang J, Zhu Y, Chen L, Ding F, Zhou R, et al. Clinical characteristics of non-critically ill patients with novel coronavirus infection (COVID-19) in a Fangcang Hospital. *Clinical Microbiology and Infection*. 2020; 26(8): 1063-1068.

[29] Mancuso M, Eikenberry SE, Gumel AB. Will vaccine-derived protective immunity curtail COVID-19 variants in the US? *Infectious Disease Modelling*. 2021; 6: 1110-1134.

[30] Inglesby TV. Public health measures and the reproduction number of SARS-CoV-2. *Jama*. 2020; 323(21): 2186-2187.

[31] Van den Driessche P, Watmough J. Reproduction numbers and sub-threshold endemic equilibria for compartmental models of disease transmission. *Mathematical Biosciences*. 2002; 180(1-2): 29-48.

[32] Heesterbeek JAP. A brief history of R_0 and a recipe for its calculation. *Acta Biotheoretica*. 2002; 50(3): 189-204. Available from: https://doi.org/10.1023/A:1016599411804.

[33] Wangari IM. Condition for global stability for a SEIR model incorporating exogenous reinfection and primary infection mechanisms. *Computational and Mathematical Methods in Medicine*. 2020; 2020(1): 9435819. Available from: https://doi.org/10.1155/2020/9435819.

[34] Castillo-Chavez C, Feng Z, Huang W. On the computation of ro and its role on global stability. In: Castillo-Chavez PC, Blower S, Driessche P, Kirschner D, Yakubu A-A. (eds.) *Mathematical Approaches for Emerging and Reemerging Infectious Diseases: An Introduction*. Springer, Berlin; 2002. p.229. Available from: https://doi.org/10.1007/978-1-4757-3667-0_13.

[35] Danchin R. *Equations différentielles l3 mathématiques*. 2011. Available from: https://perso.math.u-pem.fr/-danchin.raphael/cours/equadiff.pdf.

[36] Berhe HW, Makinde OD, Theuri DM. Parameter estimation and sensitivity analysis of dysentery diarrhea epidemic model. *Journal of Applied Mathematics*. 2019; 2019(1): 8465747.

[37] Suandi D, Ningrum IP, Alifah AN, Izzah N, Reza MP, Muwahidah IK. Mathematical modeling and sensitivity analysis of the existence of male calico cats population based on cross breeding of all coat colour types. *Communication in Biomathematical Sciences*. 2019; 2(2): 96-104.

[38] Nainggolan J, Ansori M. Stability and sensitivity analysis of the COVID-19 spread with comorbid diseases. *Symmetry*. 2022; 14(11): 2269.

[39] Tovissodé CF, Doumatè JT, Glèlè Kakaï R. A hybrid modeling technique of epidemic outbreaks with application to COVID-19 dynamics in west africa. *Biology*. 2021; 10(5): 365.

[40] Sharbayta SS, Desta HD, Abdi T. Mathematical modelling of COVID-19 transmission dynamics with vaccination: A case study in Ethiopia. *Discrete Dynamics in Nature and Society*. 2023; 2023(1): 2972164. Available from: https://doi.org/10.1155/2023/2972164.

[41] Zhao S, Musa SS, Fu H, He D, Qin J. Simple framework for real-time forecast in a data-limited situation: The Zika virus (ZIKV) outbreaks in Brazil from 2015 to 2016 as an example. *Parasites & Vectors*. 2019; 12(1): 1-13.

[42] He D, Gao D, Lou Y, Zhao S, Ruan S. A comparison study of Zika virus outbreaks in French Polynesia, Colombia and the State of Bahia in Brazil. *Scientific Reports*. 2017; 7(1): 1-6.

[43] Wang L, Li J, Guo S, Xie N, Yao L, Cao Y, et al. Real-time estimation and prediction of mortality caused by COVID-19 with patient information based algorithm. *Science of the Total Environment*. 2020; 727: 138394.

[44] Deressa CT, Duressa GF. Modeling and optimal control analysis of transmission dynamics of COVID-19: The case of Ethiopia. *Alexandria Engineering Journal*. 2021; 60(1): 719-732.

[45] Perez L, Dragicevic S. An agent-based approach for modeling dynamics of contagious disease spread. *International Journal of Health Geographics*. 2009; 8(1): 1-17.

[46] Taboe HB, Asare-Baah M, Yesmin A, Ngonghala CN. The impact of age structure and vaccine prioritization on COVID-19 in West Africa. *Infectious Disease Modelling*. 2022; 7(4): 709-727.

[47] Davies NG, Kucharski AJ, Eggo RM, Gimma A, Edmunds WJ, Jombart T, et al. Effects of non-pharmaceutical interventions on COVID-19 cases, deaths, and demand for hospital services in the UK: A modelling study. *The Lancet Public Health*. 2020; 5(7): e375-e385.

[48] Rabiu M, Iyaniwura SA. Assessing the potential impact of immunity waning on the dynamics of COVID-19 in South Africa: An endemic model of COVID-19. *Nonlinear Dynamics*. 2022; 109(1): 203-223.

[49] Ruktanonchai NW, Floyd J, Lai S, Ruktanonchai CW, Sadilek A, Rente-Lourenco P, et al. Assessing the impact of coordinated COVID-19 exit strategies across Europe. *Science*. 2020; 369(6510): 1465-1470.

[50] Edholm CJ, Levy B, Spence L, Agusto FB, Chirove F, Chukwu CW, et al. A vaccination model for COVID-19 in Gauteng, South Africa. *Infectious Disease Modelling*. 2022; 7(3): 333-345.

[51] Townsend JP, Hassler HB, Sah P, Galvani AP, Dornburg A. The durability of natural infection and vaccine-induced immunity against future infection by SARS-CoV-2. *Proceedings of the National Academy of Sciences*. 2022; 119(31): e2204336119.

[52] Dan JM, Mateus J, Kato Y, Hastie KM, Yu ED, Faliti CE, et al. Immunological memory to SARS-CoV-2 assessed for up to 8 months after infection. *Science*. 2021; 371(6529): eabf4063.

[53] Curley B. How long does immunity from COVID-19 vaccination last? *Healthline*. 2021; 855.

[54] Xin H, Li Y, Wu P, Li Z, Lau EH, Qin Y, et al. Estimating the latent period of coronavirus disease 2019 (COVID-19). *Clinical Infectious Diseases*. 2022; 74(9): 1678-1681.

[55] Parry H, Tut G, Bruton R, Faustini S, Stephens C, Saunders P, et al. mRNA vaccination in people over 80 years of age induces strong humoral immune responses against SARS-CoV-2 with cross neutralization of P. 1 Brazilian variant. *Elife*. 2021; 10: e69375.

Appendix

A.1 *Tables of fixed model parameters; countries names per region and varying per countries parameters*

Table 4. Value of the fixed model parameters

Parameter	Value	References
d_u	1/180	[51]
d_v	1/180	[52]
ω	1/180	[53]
α_e	1/5.5	[54]
α_p	1/3.2	[12]
ρ_1	0.6	[29]
ρ_2	0.1	[55]
$\gamma_{a_1}(\gamma_{a_2})$	1/5 (1/2.7)	[51]
$\gamma_{s_1}(\gamma_{s_2})$	1/10 (1/8)	[51]
$\gamma_{c_1}(\gamma_{c_2})$	1/11 (1/10)	[51]

Table 5. Countries selected per region with their vaccination start date

Region	Selected Countries	Vaccination Start date
Central	Democratic Republic of Congo (DRC) Gabon	2021-05-25 2021-03-31
Eastern	Rwanda Lybia	2021-03-05 2021-04-21
Northern	Kenya Algeria	2021-02-19 2021-01-30
Southern	Namibia South Africa (South A.)	2021-03-25 2021-02-18
Western	Benin Nigeria	2021-05-12 2021-03-15

Parameters	Countries									
	Namibia	South A.	Rwanda	Libya	DRC	Nigeria	Benin	Algeria	Gabon	Kenya
b_{uu}	0.6694	0.7413	0.5268	0.3456	0.5925	0.6308	0.8862	0.7990	0.6977	0.6392
b_{uv}	0.4698	0.4048	0.3296	0.1877	0.2562	0.4683	0.3658	0.4440	0.1996	0.6995
b_{vu}	0.4994	0.6343	0.3447	0.6354	0.2997	0.5005	0.8170	0.5470	0.1000	0.4969
b_{vv}	0.0992	0.0990	0.1871	0.0806	0.0133	0.0880	0.0249	0.0562	0.0618	0.0408
θ_{p_u}	0.9499	0.9426	0.4965	0.9735	0.9999	1.1e-04	0.2065	0.9583	0.4965	0.4616
θ_{a_u}	0.2462	0.3275	0.3610	0.5431	0.4269	0.1072	0.9893	0.3630	0.5901	0.2427
θ_{s_u}	1.1e-04	0.1175	0.4358	0.5100	0.0033	0.5197	0.2914	0.2222	0.4671	0.3168
θ_{c_u}	5.8e-06	0.2812	0.4106	0.8762	0.1070	0.7108	0.7057	0.1791	0.2670	0.0821
θ_{p_v}	0.6898	0.6939	0.4820	0.4907	0.2284	0.1718	0.7775	0.2346	0.1016	0.4551
θ_{a_v}	0.2790	0.5936	0.4979	0.4720	0.0172	0.2692	0.5197	0.4848	0.2940	0.2532
θ_{s_v}	0.1641	0.0050	0.3727	0.5913	0.4898	0.0556	0.9498	0.6214	0.1993	0.3950
θ_{c_v}	0.6778	0.2163	0.0373	0.3785	0.4097	0.0327	0.8935	0.7306	0.1944	0.0043
q_{p_1}	0.0022	0.0049	0.0001	0.0048	7.3e-04	5.3e-06	1.0e-04	0.0016	4.9e-04	1.9e-04
q_{p_2}	6.0e-04	0.0013	9.8e-05	0.0013	2.8e-04	0.0011	9.0e-05	8.0e-05	1.4e-04	5.6e-05
q_{a_1}	0.0049	0.0049	0.0025	0.0035	9.5e-04	1.4e-04	1.4e-04	2.5e-04	4.9e-04	0.0028
q_{a_2}	0.0039	0.0025	0.0018	0.0025	9.7e-04	0.0031	9.3e-05	2.9e-05	1.0e-04	0.0019
q_{s_1}	0.0086	0.0083	1.7e-04	0.0086	8.5e-06	1.0e-04	4.0e-04	0.0013	7.4e-04	0.0019
q_{s_2}	0.0029	0.0035	9.1e-04	0.0043	8.3e-06	0.0048	4.1e-04	0.0034	3.4e-04	0.0019
δ_{s_1}	2.9e-04	0.1970	2.2e-05	0.0019	2.6e-04	2.8e-04	9.8e-04	2.4e-04	2.9e-04	2.9e-04
δ_{s_2}	1.9e-04	0.0958	1.9e-04	9.9e-04	6.0e-07	0.0085	2.8e-04	1.6e-04	1.8e-04	1.1e-04
δ_{c_1}	3.9e-04	0.1995	2.0e-04	0.0019	2.9e-04	0.0093	2.9e-04	5.1e-04	1.9e-04	1.3e-04
δ_{c_2}	1.9e-05	0.0227	1.9e-04	9.9e-04	1.8e-05	0.0073	9.9e-05	2.1e-05	9.9e-05	5.5e-05
μ	4.221e-05	4.219e-05	3.911e-05	3.731e-05	4.445e-05	4.911e-05	0.0003e-05	3.533e-05	4.085e-05	4.061e-05
ν	0.00056	0.00101	0.00125	0.00107	0.00001	0.00015	0.000133	0.00085	0.00075	0.00045
Λ	264.94	4999.12	1424.7	433.56	17591.2	39787.8	2591.9	6227.6	413.61	10285.0
ψ_u	0.30	0.45	0.45	0.35	0.30	0.45	0.30	0.35	0.30	0.15
ψ_v	0.25	0.45	0.25	0.25	0.25	0.25	0.30	0.25	0.30	0.18
Initial conditions										
$S_u(0)(\times 10^4)$	166.34	4487.12	1335.27	419.45	714.87	4994.65	589.74	958.35	187.55	432.98
$E_u(0)$	1500.00	4763.61	3191.59	10043.62	69889.75	76207.26	506.92	93208.19	500.37	77571.99
$I_{P_u}(0)$	700.15	5499.92	1120.60	7097.94	1002.16	39377.52	150.36	4344.26	50.099	44589.27
$I_{A_u}(0)$	706.06	1322.84	1011.78	5144.0	541.19	12989.71	151.03	530.67	70.85	34186.64
$I_{S_u}(0)$	700.00	265.16	741.58	2500.26	784.58	571.77	228.45	581.77	314.67	13641.08
$R_u(0)$	144.62	455.28	251.03	1159.89	249.44	249.44	99.95	100.51	130.30	962.79
Reproduction numbers										
R_o	2.569	3.131	2.817	2.586	2.407	3.157	4.04	3.640	3.74	2.438
R_c	1.713	1.500	1.806	1.432	1.682	1.599	2.79	1.902	2.37	1.91

A.2 *Analytical expressions of $S_u(t)$ and $S_v(t)$*

$$S_u(t) = S_v(0)\left(\frac{\sigma_3\sigma_6\left(\omega-\mu+\sigma_{43}\right)}{2\sigma_{43}} + \frac{\sigma_4\sigma_5\left(\mu-\omega+\sigma_{43}\right)}{2\sigma_{43}}\right) - S_u(0)\left(\frac{\nu\sigma_3\sigma_6}{\sigma_{43}} - \frac{\nu\sigma_4\sigma_5}{\sigma_{43}}\right) - \frac{\Lambda\sigma_1}{\sigma_{43}} + \frac{\Lambda\sigma_2}{\sigma_{43}} + \sigma_{28} - \sigma_{23}$$

$$- \frac{\Lambda\omega\sigma_{35}}{\sigma_{43}} + \frac{K_2 d_v\sigma_{36}\sigma_1}{2\nu} + \frac{K_2 d_v\sigma_{36}\sigma_2}{2\nu} - \frac{K_1 d_u\sigma_{34}\sigma_1}{\sigma_{43}} + \frac{K_1 d_u\sigma_{34}\sigma_2}{\sigma_{43}} + \frac{K_1 d_v\sigma_{36}\sigma_1}{\sigma_{33}} + \frac{K_1 d_v\sigma_{36}\sigma_2}{\sigma_{33}}$$

$$- \sigma_{22} - \frac{K_1 d_v\sigma_{34}\sigma_1}{\sigma_{33}} - \frac{K_1 d_v\sigma_{34}\sigma_2}{\sigma_{33}} - \sigma_{25} - \frac{K_1 d_v\omega\sigma_{34}\sigma_{35}}{\sigma_{33}} + \frac{\sigma_{24}}{2\nu} + \frac{\sigma_{24}}{2\sigma_{43}} - \sigma_{27} - \frac{K_1 du\omega\sigma_{34}\sigma_{35}}{\sigma_{43}}$$

$$+ \sigma_{26} - \sigma_{18} - \sigma_{15} + \frac{K_1 d_v\omega\sigma_{36}\sigma_{35}}{\sigma_{33}} + \frac{K_1 d_v\omega^2\sigma_{36}\sigma_{35}}{\sigma_{32}} + \frac{K_1 d_v\mu\sigma_{34}\sigma_1}{\sigma_{32}} - \frac{K_1 d_v\mu\sigma_{34}\sigma_2}{\sigma_{32}} - \frac{K_1 d_v\omega\sigma_{34}\sigma_1}{\sigma_{32}}$$

$$+ \frac{K_1 d_v\omega\sigma_{34}\sigma_2}{\sigma_{32}} - \frac{K_2 d_v\mu\sigma_{36}\sigma_1}{2\nu\sigma_{43}} + \frac{K_2 d_v\mu\sigma_{36}\sigma_2}{2\nu\sigma_{43}} + \frac{K_2 d_v\omega\sigma_{36}\sigma_1}{2\nu\sigma_{43}} - \frac{K_2 d_v\omega\sigma_{36}\sigma_2}{2\nu\sigma_{43}} - \frac{K_1 d_v\omega^2\sigma_{34}\sigma_{35}}{\sigma_{32}}$$

$$+ \frac{K_2 d_v\omega^2\sigma_{36}\sigma_{35}}{2\nu\sigma_{43}} - \frac{K_1 d_v\mu\sigma_{36}\sigma_1}{\sigma_{32}} + \frac{K_1 d_v\mu\sigma_{36}\sigma_2}{\sigma_{32}} + \frac{K_1 d_v\omega\sigma_{36}\sigma_1}{\sigma_{32}} - \frac{K_1 d_v\omega\sigma_{36}\sigma_2}{\sigma_{32}} - \sigma_{21}$$

$$- \frac{K_1 d_v\mu\omega\sigma_{36}\sigma_{35}}{\sigma_{32}} + \sigma_{19} - \sigma_9 - \frac{2\Lambda\omega\sigma_{40}\mathrm{e}^{-\nu t}\sigma_{39}\sigma_{31}}{\sigma_{37}\sigma_{43}} + \sigma_{20} + \frac{K_1 d_v\mu\omega\sigma_{34}\sigma_{35}}{\sigma_{32}} - \frac{K_2 d_v\mu\omega\sigma_{36}\sigma_{35}}{2\nu\sigma_{43}}$$

$$- \sigma_{16} + \sigma_{14} + \frac{K_1 d_v\omega\sigma_{40}\mathrm{e}^{-\nu t}\sigma_{39}\sigma_{34}\sigma_{31}}{\sigma_{30}} - \frac{\sigma_{17}}{\nu\sigma_{37}} - \sigma_8 + \frac{\sigma_{17}}{\sigma_{37}\sigma_{43}} - \sigma_7 - \frac{2K_1 d_u\omega\sigma_{40}\mathrm{e}^{-\nu t}\sigma_{39}\sigma_{34}\sigma_{31}}{\sigma_{37}\sigma_{43}}$$

$$- \frac{K_1 d_v\omega\sigma_{36}\sigma_{40}\mathrm{e}^{-\nu t}\sigma_{39}\sigma_{31}}{\sigma_{30}} - \frac{K_1 d_v\omega^2\sigma_{40}\mathrm{e}^{-\nu t}\sigma_{39}\sigma_{34}\sigma_{31}}{\sigma_{29}} + \frac{K_2 d_v\omega^2\sigma_{36}\sigma_{40}\mathrm{e}^{-\nu t}\sigma_{39}\sigma_{31}}{\nu\sigma_{37}\sigma_{43}}$$

$$+ \frac{K_1 d_v\omega^2\sigma_{36}\sigma_{40}\mathrm{e}^{-\nu t}\sigma_{39}\sigma_{31}}{\sigma_{29}} + \sigma_{12} + \frac{K_1 d_v\mu\omega\sigma_{40}\mathrm{e}^{-\nu t}\sigma_{39}\sigma_{34}\sigma_{31}}{\sigma_{29}} - \sigma_{10} - \frac{K_2 d_v\mu\omega\sigma_{36}\sigma_{40}\mathrm{e}^{-\nu t}\sigma_{39}\sigma_{31}}{\nu\sigma_{37}\sigma_{43}}$$

$$- \sigma_{13} + \sigma_{11} - \frac{K_1 d_v\mu\omega\sigma_{36}\sigma_{40}\mathrm{e}^{-\nu t}\sigma_{39}\sigma_{31}}{\nu\sigma_{37}}.$$

$$S_v(t) = S_v(0)\left(\frac{\sigma_3\left(\omega-\mu+\sigma_{43}\right)}{2\sigma_{43}} + \frac{\sigma_4\left(\mu-\omega+\sigma_{43}\right)}{2\sigma_{43}}\right) - S_u(0)\left(\frac{\nu\sigma_3}{\sigma_{43}} - \frac{\nu\sigma_4}{\sigma_{43}}\right) + \sigma_{28} - \sigma_{23} - \sigma_{25} - \sigma_{22} + \frac{\sigma_{24}}{2\sigma_{43}} - \sigma_{27}$$

$$+ \sigma_{26} - \sigma_{21} + \sigma_{19} - \sigma_9 + \sigma_{20} - \sigma_{18} - \sigma_{16} + \sigma_{14} - \sigma_8 + \frac{\sigma_{17}}{\sigma_{37}\sigma_{43}} - \sigma_7 - \sigma_{15} + \sigma_{12} - \sigma_{10} - \sigma_{13} + \sigma_{11}.$$

where,

$$\sigma_1 = \sigma_{41}\sigma_{40}e^{-\nu t}\sigma_{39} - 1; \qquad \sigma_2 = \sigma_{38}\sigma_{40}e^{-\nu t}\sigma_{39} - 1; \qquad \sigma_3 = e^{-t\left(\frac{\mu+\omega+2\nu+\sigma_{43}}{2}\right)};$$

$$\sigma_4 = e^{t\left(\frac{-\mu-\omega-2\nu+\sigma_{43}}{2}\right)}; \qquad \sigma_5 = \frac{-\nu+\omega+\sigma_{43}}{2}; \qquad \sigma_6 = \frac{-\nu+\omega-\sigma_{43}}{2};$$

$$\sigma_7 = \frac{2K_1 d_u \nu \sigma_{40}e^{-\nu t}\sigma_{39}\sigma_{34}\sigma_{31}}{\sigma_{37}\sigma_{43}}; \qquad \sigma_8 = \frac{K_2 d_v \mu \sigma_{36}\sigma_{40}e^{-\nu t}\sigma_{39}\sigma_{31}}{\sigma_{37}\sigma_{43}}; \qquad \sigma_9 = \frac{2\Lambda\nu\sigma_{40}e^{-\nu t}\sigma_{39}\sigma_{31}}{\sigma_{37}\sigma_{43}};$$

$$\sigma_{10} = \frac{K_1 d_v \nu\omega\sigma_{40}e^{-\nu t}\sigma_{39}\sigma_{34}\sigma_{31}}{\sigma_{29}}; \qquad \sigma_{11} = \frac{K_1 d_v \nu\omega\sigma_{36}\sigma_{40}e^{-\nu t}\sigma_{39}\sigma_{31}}{\sigma_{29}}; \qquad \sigma_{12} = \frac{K_1 d_v \mu\nu\sigma_{40}e^{-\nu t}\sigma_{39}\sigma_{34}\sigma_{31}}{\sigma_{29}};$$

$$\sigma_{13} = \frac{K_1 d_v \mu\nu\sigma_{36}\sigma_{40}e^{-\nu t}\sigma_{39}\sigma_{31}}{\sigma_{29}}; \qquad \sigma_{14} = \frac{K_1 d_v \nu\sigma_{40}e^{-\nu t}\sigma_{39}\sigma_{34}\sigma_{31}}{\sigma_{30}}; \qquad \sigma_{15} = \frac{K_1 d_v \nu\sigma_{36}\sigma_{40}e^{-\nu t}\sigma_{39}\sigma_{31}}{\sigma_{30}};$$

$$\sigma_{16} = \frac{K_2 d_v \sigma_{36}\sigma_{40}e^{-\nu t}\sigma_{39}\sigma_{31}}{\sigma_{37}}; \qquad \sigma_{17} = K_2 d_v \omega\sigma_{36}\sigma_{40}e^{-\nu t}\sigma_{39}\sigma_{31}; \qquad \sigma_{18} = \frac{K_1 d_v \nu\omega\sigma_{34}\sigma_{35}}{\sigma_{32}};$$

$$\sigma_{19} = \frac{K_1 d_v \nu\omega\sigma_{36}\sigma_{35}}{\sigma_{32}}; \qquad \sigma_{20} = \frac{K_1 d_v \mu\nu\sigma_{34}\sigma_{35}}{\sigma_{32}}; \qquad \sigma_{21} = \frac{K_1 d_v \mu\nu\sigma_{36}\sigma_{35}}{\sigma_{32}};$$

$$\sigma_{22} = \frac{K_2 d_v \mu\sigma_{36}\sigma_{35}}{2\sigma_{43}}; \qquad \sigma_{23} = \frac{\Lambda\nu\sigma_{35}}{\sigma_{43}}; \qquad \sigma_{24} = K_2 d_v \omega\sigma_{36}\sigma_{35};$$

$$\sigma_{25} = \frac{K_1 d_v \nu\sigma_{34}\sigma_{35}}{\sigma_{33}}; \qquad \sigma_{26} = \frac{K_1 d_v \nu\sigma_{36}\sigma_{35}}{\sigma_{33}}; \qquad \sigma_{27} = \frac{K_1 d_u \nu\sigma_{34}\sigma_{35}}{\sigma_{43}};$$

$$\sigma_{28} = \frac{K_2 d_v \sigma_{36}\sigma_{35}}{2}; \qquad \sigma_{29} = (d_u - d_v + \nu)\sigma_{37}\sigma_{43}; \qquad \sigma_{30} = (d_u - d_v + \nu)\sigma_{37};$$

$$\sigma_{31} = \sigma_{38} - e^{t\left(\frac{\mu+2\nu+\omega}{2}\right)}; \qquad \sigma_{32} = 2(d_u - d_v + \nu)\sigma_{43}; \qquad \sigma_{33} = 2(d_u - d_v + \nu);$$

$$\sigma_{34} = e^{-t(d_u+\mu+\nu)}; \qquad \sigma_{35} = \frac{2(1-\sigma_{41}\sigma_{40}e^{-\nu t}\sigma_{39})}{\sigma_{42}}; \qquad \sigma_{36} = e^{-t(d_v+\mu)};$$

$$\sigma_{37} = \mu + 2\nu + \omega - \sigma_{43}; \qquad \sigma_{38} = e^{\frac{t\sigma_{43}}{2}}; \qquad \sigma_{39} = e^{-\frac{\omega t}{2}};$$

$$\sigma_{40} = e^{-\frac{\mu t}{2}}; \qquad \sigma_{41} = e^{-\frac{t\sigma_{43}}{2}}; \qquad \sigma_{42} = \mu + 2\nu + \omega + \sigma_{43} \text{ and}$$

$$\sigma_{43} = \sqrt{(\mu-\omega)^2 + 4\nu\omega}.$$

A.3 *Analytical expressions of matrices J_{11}, J_{12}, J_{13} and J_{14}*

$$J_{11} = \begin{bmatrix} -\frac{L_1}{N'} + \frac{L_1 S_u}{N'^2} - \mu - \nu & \frac{L_1 S_u}{N'^2} & -S_u\left(-\frac{L_1}{N'^2} + \frac{b_{uu}\theta_{pu}(1-\psi_u)}{N'}\right) & -S_u\left(-\frac{L_1}{N'^2} + \frac{b_{uu}\theta_{au}(1-\psi_u)}{N'}\right) \\ \frac{L_1}{N'} - \frac{L_1 S_u}{N'^2} & -\frac{L_1 S_u}{N'^2} - a_1 & -\frac{L_1 S_u}{N'^2} + \frac{S_u b_{uu}\theta_{pu}(1-\psi_u)}{N'} & -\frac{L_1 S_u}{N'^2} + \frac{S_u b_{uu}\theta_{au}(1-\psi_u)}{N'} \\ 0 & \alpha_e & -a_2 & 0 \\ 0 & 0 & \alpha_p(1-\rho_1) & -a_3 \\ 0 & 0 & \alpha_p\rho_1 & 0 \\ 0 & 0 & q_{p1} & q_{a1} \\ 0 & 0 & 0 & 0 \\ 0 & 0 & 0 & \gamma_{a1} \\ \frac{L_2 S_v}{N'^2} + \nu & \frac{L_2 S_v}{N'^2} & -S_v\left(-\frac{L_2}{N'^2} + \frac{b_{uv}\theta_{pu}(1-\psi_u)}{N'}\right) & -S_v\left(-\frac{L_2}{N'^2} + \frac{b_{uv}\theta_{au}(1-\psi_u)}{N'}\right) \\ -\frac{L_2 S_v}{N'^2} & -\frac{L_2 S_v}{N'^2} + \nu & -\frac{L_2 S_v}{N'^2} + \frac{S_v b_{uv}\theta_{pu}(1-\psi_u)}{N'} & -\frac{L_2 S_u}{N'^2} + \frac{S_v b_{uv}\theta_{au}(1-\psi_u)}{N'} \\ 0 & 0 & \nu & 0 \\ 0 & 0 & 0 & \nu \\ 0 & 0 & 0 & 0 \\ 0 & 0 & 0 & 0 \\ 0 & 0 & 0 & 0 \\ 0 & 0 & 0 & 0 \\ 0 & 0 & 0 & 0 \end{bmatrix}$$

$$J_{12} = \begin{bmatrix} -S_u\left(-\frac{L_1}{N'^2} + \frac{b_{uu}\theta_{su}(1-\psi_u)}{N'}\right) & -S_u\left(-\frac{L_1}{N'^2} + \frac{b_{uu}\theta_{cu}(1-\psi_u)}{N'}\right) & \frac{L_1 S_u}{N'^2} & \frac{L_1 S_u}{N'^2} + d_u \\ -\frac{L_1 S_u}{N'^2} + \frac{S_u b_{uu}\theta_{su}(1-\psi_u)}{N'} & -\frac{L_1 S_u}{N'^2} + \frac{S_u b_{uu}\theta_{cu}(1-\psi_u)}{N'} & -\frac{L_1 S_u}{N'^2} & -\frac{L_1 S_u}{N'^2} \\ 0 & 0 & 0 & 0 \\ 0 & 0 & 0 & 0 \\ -a_4 & 0 & 0 & 0 \\ q_{s1} & -a_5 & 0 & 0 \\ \delta_{s1} & \delta_{c1} & 0 & 0 \\ \gamma_{c1} & \gamma_{c1} & 0 & -d_u - \mu - \nu \\ -S_v\left(-\frac{L_2}{N'^2} + \frac{b_{uv}\theta_{su}(1-\psi_u)}{N'}\right) & -S_v\left(-\frac{L_2}{N'^2} + \frac{b_{uv}\theta_{cu}(1-\psi_u)}{N'}\right) & \frac{L_2 S_v}{N'^2} & \frac{L_2 S_v}{N'^2} \\ \gamma_{s1} & -\frac{L_2 S_u}{N'^2} + \frac{S_v b_{uv}\theta_{cu}(1-\psi_u)}{N'} & -\frac{L_2 S_u}{N'^2} & -\frac{L_2 S_u}{N'^2} \\ 0 & 0 & 0 & 0 \\ 0 & 0 & 0 & 0 \\ 0 & 0 & 0 & 0 \\ 0 & 0 & 0 & 0 \\ 0 & 0 & 0 & 0 \\ 0 & 0 & 0 & 0 \end{bmatrix} ;$$

$$J_{13} = \begin{bmatrix}
\frac{L_1 S_u}{N'^2} + \omega & \frac{L_1 S_u}{N'^2} & -S_u\left(-\frac{L_1}{N'^2} + \frac{b_{vu}\theta_{pv}(1-\psi_v)}{N'}\right) & -S_u\left(-\frac{L_1}{N'^2} + \frac{b_{vu}\theta_{av}(1-\psi_v)}{N'}\right) \\[4pt]
-\frac{L_1 S_u}{N'^2} & -\frac{L_1 S_u}{N'^2} & -\frac{L_1 S_u}{N'^2} + \frac{S_u b_{vu}\theta_{pv}(1-\psi_v)}{N'} & -\frac{L_1 S_{uv}}{N'^2} + \frac{S_u b_{vu}\theta_{av}(1-\psi_v)}{N'} \\[4pt]
0 & 0 & 0 & 0 \\
0 & 0 & 0 & 0 \\
0 & 0 & 0 & 0 \\
0 & 0 & 0 & 0 \\
0 & 0 & 0 & 0 \\
0 & 0 & 0 & 0 \\
-\frac{L_2}{N'} + \frac{L_2 S_v}{N'^2} - \mu - \omega & \frac{L_2 S_v}{N'^2} & -S_v\left(-\frac{L_2}{N'^2} + \frac{b_{vv}\theta_{pv}(1-\psi_v)}{N'}\right) & -S_v\left(-\frac{L_2}{N'^2} + \frac{b_{vv}\theta_{av}(1-\psi_v)}{N'}\right) \\[4pt]
\frac{L_2}{N'} - \frac{L_2 S_v}{N'^2} & -\frac{L_2 S_v}{N'^2} - a_6 & -\frac{L_2 S_v}{N'^2} + \frac{S_v b_{vv}\theta_{pv}(1-\psi_v)}{N'} & -\frac{L_2 S_v}{N'^2} + \frac{S_v b_{vv}\theta_{av}(1-\psi_v)}{N'} \\[4pt]
0 & \alpha_e & -a_7 & 0 \\
0 & 0 & \alpha_p(1-\rho_2) & -a_8 \\
0 & 0 & \alpha_p\rho_2 & 0 \\
0 & 0 & q_{p2} & q_{a2} \\
0 & 0 & 0 & 0 \\
0 & 0 & 0 & \gamma_{a2}
\end{bmatrix} ;$$

$$J_{14} = \begin{bmatrix}
-S_u\left(-\frac{L_1}{N'^2} + \frac{b_{vu}\theta_{sv}(1-\psi_v)}{N'}\right) & -S_u\left(-\frac{L_1}{N'^2} + \frac{b_{uu}\theta_{cu}(1-\psi_v)}{N'}\right) & \frac{L_1 S_u}{N'^2} & \frac{L_1 S_u}{N'^2} \\[4pt]
-\frac{L_1 S_u}{N'^2} + \frac{S_u b_{vu}\theta_{sv}(1-\psi_v)}{N'} & -\frac{L_1 S_u}{N'^2} + \frac{S_u b_{vu}\theta_{uv}(1-\psi_v)}{N'} & -\frac{L_1 S_u}{N'^2} & -\frac{L_1 S_u}{N'^2} \\[4pt]
0 & 0 & 0 & 0 \\
0 & 0 & 0 & 0 \\
0 & 0 & 0 & 0 \\
0 & 0 & 0 & 0 \\
0 & 0 & 0 & 0 \\
0 & 0 & 0 & 0 \\
-S_v\left(-\frac{L_2}{N'^2} + \frac{b_{vv}\theta_{sv}(1-\psi_v)}{N'}\right) & -S_v\left(-\frac{L_2}{N'^2} + \frac{b_{vv}\theta_{cv}(1-\psi_v)}{N'}\right) & \frac{L_2 S_v}{N'^2} & \frac{L_2 S_v}{N'^2} + d_v \\[4pt]
-\frac{L_2 S_v}{N'^2} + \frac{S_v b_{vv}\theta_{sv}(1-\psi_v)}{N'} & -\frac{L_2 S_v}{N'^2} + \frac{S_v b_{vv}\theta_{cv}(1-\psi_v)}{N'} & -\frac{L_2 S_v}{N'^2} & -\frac{L_2 S_v}{N'^2} \\[4pt]
0 & 0 & 0 & 0 \\
0 & 0 & 0 & 0 \\
-a_9 & 0 & 0 & 0 \\
q_{s2} & -a_0 & 0 & 0 \\
\delta_{s2} & \delta_{c2} & 0 & 0 \\
\gamma_{s2} & \gamma_{c2} & 0 & -d_v - \mu
\end{bmatrix} .$$

$$L_1 = (1-\psi_u)\, b_{uu}\left(\theta_{p_u}I_{P_u} + \theta_{a_u}I_{A_u} + \theta_{s_u}I_{Su} + \theta_{c_u}C_u\right) + (1-\psi_v)\, b_{vu}\left(\theta_{p_v}I_{P_v} + \theta_{a_v}I_{A_v} + \theta_{s_v}I_{S_v} + \theta_{c_v}C_v\right)$$

$$L_2 = (1-\psi_v)\, b_{vv}\left(\theta_{p_v}I_{P_v} + \theta_{a_v}I_{A_v} + \theta_{s_v}I_{S_v} + \theta_{c_v}C_v\right) + (1-\psi_u)\, b_{uv}\left(\theta_{p_u}I_{P_u} + \theta_{a_u}I_{A_u} + \theta_{s_u}I_{S_u} + \theta_{c_u}C_u\right)$$

$$N' = C_u + C_v + D_u + D_v + E_u + E_v + I_{A_u} + I_{A_v} + I_{P_u} + I_{P_v} + I_{S_u} + I_{S_v} + R_u + R_v + S_u + S_v$$